

AEDC-TR-91-12

Copy 3

**Signal Conditioning of Single-Active-Arm
Strain Gages Used for
Dynamic Stress Measurement**

**B. G. Mahrenholz
Sverdrup Technology, Inc., AEDC Group**

September 1991

Final Report for Period October 1, 1989 to June 30, 1991

Approved for public release; distribution is unlimited.

**PROPERTY OF U.S. AIR FORCE
AEDC TECHNICAL LIBRARY**

**TECHNICAL REPORTS
FILE COPY**

**ARNOLD ENGINEERING DEVELOPMENT CENTER
ARNOLD AIR FORCE BASE, TENNESSEE
AIR FORCE SYSTEMS COMMAND
UNITED STATES AIR FORCE**



NOTICES

When U. S. Government drawings, specifications, or other data are used for any purpose other than a definitely related Government procurement operation, the Government thereby incurs no responsibility nor any obligation whatsoever, and the fact that the Government may have formulated, furnished, or in any way supplied the said drawings, specifications, or other data, is not to be regarded by implication or otherwise, or in any manner licensing the holder or any other person or corporation, or conveying any rights or permission to manufacture, use, or sell any patented invention that may in any way be related thereto.

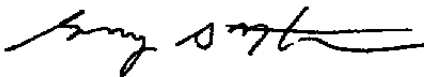
Qualified users may obtain copies of this report from the Defense Technical Information Center.

References to named commercial products in this report are not to be considered in any sense as an endorsement of the product by the United States Air Force or the Government.

This report has been reviewed by the Office of Public Affairs (PA) and is releasable to the National Technical Information Service (NTIS). At NTIS, it will be available to the general public, including foreign nations.

APPROVAL STATEMENT

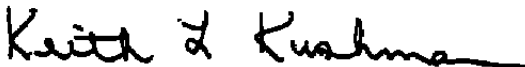
This report has been reviewed and approved.



GREGORY G. NORDSTROM, 1Lt, USAF
Propulsion Division
Directorate of Technology
Deputy for Operations

Approved for publication:

FOR THE COMMANDER



KEITH L. KUSHMAN
Technical Director
Directorate of Technology
Deputy for Operations

REPORT DOCUMENTATION PAGE			<i>Form Approved</i> OMB No. 0704-0188	
Public reporting burden for this collection of information is estimated to average 1 hour per response, including the time for reviewing instructions, searching existing data sources, gathering and maintaining the data needed, and completing and reviewing the collection of information. Send comments regarding this burden estimate or any other aspect of this collection of information, including suggestions for reducing this burden, to Washington Headquarters Services, Directorate for Information Operations and Reports, 1215 Jefferson Davis Highway, Suite 1204, Arlington, VA 22202-4302, and to the Office of Management and Budget, Paperwork Reduction Project (0704-0188), Washington, DC 20503.				
1. AGENCY USE ONLY (Leave blank)	2. REPORT DATE September 1991	3. REPORT TYPE AND DATES COVERED Final -- Oct. 1, 1989 - June 30, 1991		
4. TITLE AND SUBTITLE Signal Conditioning of Single-Active-Arm Strain Gages Used for Dynamic Stress Measurement			5. FUNDING NUMBERS PE - 65807F PR - DC97EW	
6. AUTHOR(S) Mahrenholz, B. G., Sverdrup Technology, Inc., AEDC Group				
7. PERFORMING ORGANIZATION NAME(S) AND ADDRESS(ES) Arnold Engineering Development Center/DOP Air Force Systems Command Arnold Air Force Base, TN 37389-5000			8. PERFORMING ORGANIZATION REPORT NUMBER AEDC-TR-91-12	
9. SPONSORING/MONITORING AGENCY NAME(S) AND ADDRESS(ES) Arnold Engineering Development Center/DOT Air Force Systems Command Arnold Air Force Base, TN 37389-5000			10. SPONSORING/MONITORING AGENCY REPORT NUMBER	
11. SUPPLEMENTARY NOTES Available in Defense Technical Information Center (DTIC).				
12a. DISTRIBUTION/AVAILABILITY STATEMENT Approved for public release; distribution is unlimited.			12b. DISTRIBUTION CODE	
13. ABSTRACT (Maximum 200 words) <p>A new strain-gage signal conditioner is described for use in the measurement of dynamic stresses on turbine engine compressor blades. This conditioner has two novel circuits. A new gage excitation circuit corrects for changes in lead-wire resistance by automatically adjusting resistances in series with the leads to the gage. This maintains a balanced configuration that offers better high-frequency common-mode rejection and less broadband noise than with constant-current excitation.</p> <p>Another circuit in the conditioner provides system calibration by shunting a small value resistor that is in series with the gage to produce a ΔR resistance change that accurately simulates the gage resistance change. The shunting is done at a rate of 1,000 times a second to produce a 1-kHz square-wave calibration signal. The calibration circuit may be used to check on the integrity of the gage and its cabling. The square wave may be used as a check on recording system frequency response.</p>				
14. SUBJECT TERMS signal conditioning stress measurement calibration strain gage			15. NUMBER OF PAGES 45	
			16. PRICE CODE	
17. SECURITY CLASSIFICATION OF REPORT UNCLASSIFIED	18. SECURITY CLASSIFICATION OF THIS PAGE UNCLASSIFIED	19. SECURITY CLASSIFICATION OF ABSTRACT UNCLASSIFIED	20. LIMITATION OF ABSTRACT SAME AS REPORT	

PREFACE

Recent developments in turbojet engine testing have led to the re-evaluation of the signal conditioning circuit used with single-active-arm strain gages for dynamic stress measurement. As may be expected, there is an increased demand for accuracy and extended data bandwidth. Achievement of these requirements is made more difficult by the proliferation of fast rise time digital electronic circuitry with its accompanying generation of electrical noise. Also complicating the picture is the practice of engine manufacturers using small-diameter, high-resistance thermocouple wire as lead wire for the strain gages. The resistance of this wire changes significantly with temperature and also is unbalanced between the two leads.

A new signal conditioning circuit has been developed under AEDC Air Force Project No. DC97EW that accommodates changing lead-wire resistance without loss of accuracy and still maintains low internal noise and good common-mode rejection of unwanted electrical signals. This signal conditioner also includes a novel delta-R calibration circuit that provides a more accurate simulation of actual gage resistance change.

A prototype signal conditioner has been built and evaluated in the laboratory. This report describes the prototype conditioner and presents the results of the evaluation.

CONTENTS

	<u>Page</u>
1.0 INTRODUCTION	5
1.1 Background	5
1.2 Description of the Problem	5
2.0 CONDITIONER DESIGN	6
2.1 Constant-Resistance Circuit	6
2.2 Delta-R Calibration Technique	8
2.3 Driven Shield Technique for Improved Common-Mode Rejection	11
3.0 PROTOTYPE SIGNAL CONDITIONER	12
3.1 Block Diagram	12
3.2 Mechanical Description	12
3.3 Detailed Circuit Description	13
3.4 Modifications to Pacific Power Supply Board	16
4.0 PERFORMANCE OF CONDITIONER	16
4.1 Excitation Regulation	16
4.2 Common-Mode Rejection	17
4.3 Internal Noise	18
5.0 RECOMMENDATIONS FOR USE OF CONDITIONER	19
5.1 Data Reduction Using Square-Wave Calibration Signal	19
5.2 Setup of Conditioner for Different Gage Resistances and Currents	20
5.3 Conditioner Input Wiring	20
6.0 CONCLUSION	21
REFERENCES	21

ILLUSTRATIONS

<u>Figure</u>	<u>Page</u>
1. Dynamic Stress Measurement Circuit Using Constant-Current Excitation	23
2. Equivalent of Constant-Current Excitation Source	23
3. Dynamic Stress Measurement Circuit Using Constant-Voltage Excitation	23

<u>Figure</u>	<u>Page</u>
4. Loading of Gage Output by Excitation Supply	24
5. Scheme for Lead-Wire Resistance Correction	24
6. Circuit to Correct for Lead-Wire Resistance Change	25
7. Parallel Combination of VACTROLS®	25
8. Millivolt Substitution Calibration Technique	26
9. Delta-R Calibration Scheme	26
10. Delta-R Calibration Circuit Using Power MOSFET	27
11. Effect of Unequal Lead-Wire Resistance on Common-Mode Rejection	28
12. Input Cable with Driven Shield	29
13. Block Diagram of Prototype Conditioner	29
14. Photograph of Prototype Conditioner	30
15. Calibration and Lead Correction Circuitry	31
16. Low-Noise Excitation Supply	32
17. Low-Pass Filter and Output Drivers	33
18. Calibration Control Circuitry	34
19. Power Connections and Guard Drivers	35
20. Constant-Current Regulator for Neff Signal Conditioner	36
21. Measurement of Common-Mode Rejection	36
22. Common-Mode Rejection	37
23. Measurement of Conditioner Internal Noise	38
24. Amplitude of Fundamental Component of Square Wave	39

TABLES

<u>Tables</u>	<u>Page</u>
1. Common-Mode to Normal-Mode Conversion for Circuit Shown	40
2. Regulation Accuracy	41
3. Internal Noise	41
4. Spreadsheet for Analysis of Conditioner	42

1.0 INTRODUCTION

1.1 BACKGROUND

In aeromechanical testing of developmental turbojet engines, dynamic stresses on the compressor and turbine blades are measured using resistance strain gages bonded to the blades. The resistance of these gages is typically either 120 or 350 ohms; they exhibit a change of a fraction of an ohm when they are subjected to strain levels typically encountered by the blades. Small-diameter, unshielded lead wires connect the gages to a disconnect point near the engine where permanent, shielded cabling runs to remotely located signal conditioning equipment.

Many engine manufacturers use thermocouple extension wire for the leads from the gages. Thermocouple wire is used because it is small in diameter, withstands high temperature, and is readily available. Unfortunately, thermocouple wire has a relatively high resistance that changes with temperature. During engine operation, the lead wire is subjected to large temperature excursions and the resulting resistance change affects the system sensitivity, causing error in the data. (The lead wire resistance change because of temperature may be greater than the gage resistance change caused by stress.)

1.2 DESCRIPTION OF THE PROBLEM

The approach normally used to eliminate problems with changing lead wire resistance is to use a signal conditioner having constant-current excitation. With the circuit as shown in Fig. 1, the stress signal is a-c coupled from the gage, and slowly changing lead resistances have no effect. Any change occurs at a rate below that of the data and is therefore not passed by the coupling capacitors.

Use of constant-current excitation results in other problems, however. First, the constant-current generator must respond fast enough to follow the highest frequency gage resistance variations and to keep the current through the gage constant. This requires a supply with a fast slew rate capable of driving the capacitive load of the shielded cable to the gage.

Although many constant-current supplies are capable of tracking the gage resistance variations, the wide bandwidth of such a supply presents another problem. The noise in the output of an active device is a function of the bandwidth of the device. With such a wide bandwidth, the noise produced by a constant-current supply is much greater than the corresponding noise from a signal conditioner having a constant-voltage excitation supply.

A third problem with the constant-current excitation supply is not so obvious. As shown in Fig. 2, a constant-current source normally consists of a constant-voltage supply with a constant-current regulator in series with its positive lead. Since ideally a constant-current source has an infinite impedance, the gage and its instrumentation amplifier see a very high impedance back to the excitation supply on the positive lead and a very low impedance back to the excitation supply on the negative lead. This unbalanced condition seriously impacts the common-mode rejection of the system. Conditioner manufacturers will attempt to float the excitation supply and enclose it in guard circuitry, but the common-mode performance is still inferior to that obtainable with a balanced circuit using constant-voltage excitation, especially at higher frequencies.

With the myriad of digital electronics in and near data systems, the common-mode noise seen by an instrumentation amplifier is no longer just a 60-Hz sine wave. In today's environment, it consists of broadband noise (approximating white noise) with predominant 60-Hz spikes. Common-mode rejection is important over the entire data bandwidth of the conditioner and not just the d-c to 60- or 120-Hz range specified by most signal conditioner manufacturers.

2.0 CONDITIONER DESIGN

A signal conditioner was designed that would have improved performance over available devices (Ref. 1). The work was conducted at the Arnold Engineering Development Center (AEDC), Air Force Systems Command (AFSC), under Program Element 65807F at the request of AEDC/DOT, Arnold Air Force Base, TN. The AEDC/DOT Project Manager was 1Lt. G. G. Nordstrom. Management for this project was performed by Sverdrup Technology, Inc., AEDC Group (a Sverdrup Corporation Company), operating contractor of the propulsion test facilities, AEDC, AFSC, Arnold Air Force Base, TN, under Air Force Project No. DC97EW. The Sverdrup Project Manager was Mr. T. F. Tibbals.

Three unique circuits were investigated for possible inclusion in the conditioner.

2.1 CONSTANT-RESISTANCE CIRCUIT

The problems of the constant-current excitation circuit are not present with the constant-voltage circuit shown in Fig. 3. This circuit is electrically equivalent to the conventional single-active-arm bridge circuit but has the adjacent arm split into two halves to provide a balanced condition. The circuit, however, is sensitive to changes in lead resistance, R_{LEAD} . Changes in R_{LEAD} affect the output in two ways: first, changes in R_{LEAD} will change the current through the gage, and a different output signal (ΔV) will result from the same ΔR ; second, the output seen by the recorder is a function of the voltage divider made up of $R_{LEAD1} +$

$R_{LEAD2} + R_{GAGE}$ and $R_{BALLAST1} + R_{BALLAST2}$. Consequently, as R_{LEAD} changes, the fraction of the gage output seen by the recorder changes. Figure 3 has been redrawn in Fig. 4 to better illustrate this effect.

The only way to minimize the effect of lead resistance changes is to increase the resistance values of $R_{BALLAST1}$ and $R_{BALLAST2}$. This requires a very high voltage power supply and large wattage resistors for $R_{BALLAST1}$ and $R_{BALLAST2}$. As these resistors are increased in value, circuit balance becomes more sensitive to stray resistance and capacitance, and common-mode rejection again suffers.

A modification of the constant-voltage circuit has been devised that eliminates the problem of lead-resistance changes. This modification adds variable resistors, in series with the leads to the gage, that can be automatically adjusted to keep the total lead-wire resistance constant (see Fig. 5). As long as the total loop resistance remains constant, the average current through the gage and also the loading on the gage will remain constant so the output signal from the conditioner will not change.

If the total loop resistance is constant, the voltage between points A and B in Fig. 5 will be constant. This voltage may be sensed and used to control the series resistances. Since the lead-wire resistance changes slowly with time, its resistance change can be distinguished from that of the gage, which changes very rapidly. The controlled resistances are split equally in each lead to keep a balanced condition.

Several devices were considered as candidates for the variable resistances. In theory, motor-driven, ganged potentiometers would be the perfect device. The resistance of dual pots could be made to track very closely and the response time of a motor-driven pot would be adequate since the lead-wire resistance changes very slowly. Small (0.5-in.-diam) motors and pots are now available for this application; however, utilization of these motors here would force them to continuously hunt or control, producing a shorter pot life than desired.

The next device investigated was the power MOSFET transistor. These devices have a desirably low "on" resistance and require very little power to control. An N-channel device would be required in the negative lead and a P-channel device in the positive lead. With these devices, however, isolation from the control circuit is a problem. There were also concerns about the noise produced by the devices, with the linearity of the devices, and with the resistance tracking between an N-channel and a P-channel device.

The device selected for the controlled resistance was the lamp/photoconductive cell combination manufactured by EG&G Vactec, Clairex, and others. The Vactec Model VTL5C4 VACTROL® (Ref. 2) has the lowest "on" resistance for a light-emitting diode (LED) lamp-

type device. Devices using incandescent lamps have a lower "on" resistance, but the filament of the lamp causes the device to be microphonic. Any vibration of the conditioner would result in noise on the channel.

A circuit was designed around the VTL5C4 that would include a variable resistance in series with each gage lead that could be varied between 150 and 50 ohms to accommodate lead resistances between 0 and 100 ohms. (The total resistance in each lead would always total 150 ohms.) A simplified drawing of the resultant circuit is shown in Fig. 6. The voltage difference between points A and B is sensed by the lower instrumentation amplifier and then compared against a reference voltage by the error amplifier. The output of the error amplifier is buffered by a current amplifier which drives the LEDs in the VACTROL LED/photoconductive cell devices. A capacitor on the compensation terminals of the error amplifier limits the bandwidth of the control loop so the loop will not respond to the rapid resistance changes of the gage caused by stress. The upper instrumentation amplifier supplies an a-c coupled strain signal to the data recording system.

Because the resistances of the LED lamp devices are not as low as desired, it was necessary to use two of the EG&G Vactec Model VTL5C4 devices in parallel with a 150-ohm resistor to obtain a controllable resistance range of 50-150 ohms (see Fig. 7). One of these parallel combinations is used in series with each of the two leads to the gage. By selecting VTL5C4 devices, it was possible to make the resistance of the two parallel combinations track within 1 percent over the range of 50 to 150 ohms.

In operation, if the lead resistance should increase, the voltage between points A and B of Fig. 6 will increase. This will result in a greater positive voltage into the error amplifier and a greater difference signal out. More current will then be driven through the VACTROL LEDs, reducing the resistance of the photoconductive cells and thus correcting for the increased lead resistance. Since the circuit functions by maintaining a constant resistance in each sensor lead, the circuit has been named "constant resistance." A patent application has been filed on this concept.

2.2 DELTA-R CALIBRATION TECHNIQUE

Calibration of dynamic strain-gage systems is customarily performed by voltage substitution. This technique, as shown in Fig. 8, consists of disconnecting the gage and its power supply from the input to the data instrumentation amplifier by means of a relay (shown schematically as SW_{1A} and SW_{1B}) and substituting a sine-wave signal from a calibration source. The amplitude of the calibration signal is related to stress by an involved calculation including Young's modulus, gage resistance, gage current, lead resistance, load resistance, etc. Using the circuit of Fig. 8:

$$\Delta R = \frac{(\sigma) (R_G) (GF)}{E} \quad (1)$$

$$V_{OUT} = \left(\frac{R_L + R_G}{R_B + R_L + R_G} - \frac{R_L + R_G + \Delta R}{R_B + R_L + R_G + \Delta R} \right) \cdot V_{BAT} \quad (2)$$

where

- ΔR = Resistance change of gage
- σ = Stress
- R_G = Gage resistance
- GF = Gage factor
- E = Young's modulus
- V_{OUT} = Peak-to-peak output voltage
- R_L = Total lead resistance
- R_B = Total ballast resistance
- V_{BAT} = Battery excitation voltage

To simplify the calibration process and to reduce the errors resulting from any change in lead resistance or gage excitation voltage, a different calibration scheme was adopted. This scheme uses a small resistor in series with the gage whose resistance is changed by an amount equal to the change in gage resistance produced by a given amount of strain. This relationship may be determined from the manufacturer's specifications for the strain gage using Eq. (1) above.

The delta-R calibration circuit is shown in Fig. 9; this circuit consists of a precision 10-ohm resistor in the negative excitation lead to the gage that is shunted by an R_{CAL} resistor to produce a circuit effect equal to a similar resistance change in the gage. Typically, R_{CAL} might be 390 ohms, which will produce a 0.25-ohm change. With a 120-ohm gage, a gage factor of 2.0, and a modulus of elasticity of 29.8×10^6 , 0.25 ohms represents 31.04 ksi. This calibration technique may be compared to the shunt-resistance calibration of a standard strain-gage pressure transducer. A second 10-ohm resistor is placed in the positive excitation lead to maintain circuit balance.

The data recording system is capacitively coupled and will not sustain the level resulting from a step change in resistance for any appreciable length of time. To produce a signal suitable for the recording system, the calibration switch SW_{CAL} is alternately opened and closed for 500 μ sec, generating a 1-kHz square-wave signal. The peak-to-peak value of the square wave is equivalent to the known value of peak-to-peak stress. This calibration scheme is usable with any type of strain-gage conditioner and may be used to remove any errors caused by lead-wire resistance or excitation voltage change.

Implementing the calibration scheme of Fig. 9 requires finding a fast operating switch having a low "on" resistance. There are high-speed, mercury-wetted contact reed relays that will operate at speeds approaching those required, but the life of these devices, which is quoted typically at 10^9 operations, is a limitation.

CMOS switches and JFET transistors are frequently used for switching applications where high-speed switching and essentially infinite lifetimes are required. However, the "on" resistance of these devices is 50 to 100 ohms or more, which would cause an unacceptable error when in series with the 390-ohm calibration resistor.

Power MOSFET transistors have recently become popular for use in switching-type power supplies and similar applications. These devices are designed to have an "on" resistance of less than an ohm to obtain maximum efficiency from the supplies. Although the device is designed for switching high currents, the "on" resistance of a power MOSFET actually decreases slightly at low currents. As mentioned previously, the power MOSFET requires very little power to drive: its gate appears as a capacitance. An International Rectifier Type IRF511 power MOSFET (Ref. 3) with an "on" resistance of 0.6 ohm was selected as the switching device for the calibration circuit. The 0.6-ohm resistance is insignificant compared to the 390-ohm calibration resistance and may therefore be ignored.

Because the source and drain of the power MOSFET are connected to one side of the strain gage, it is necessary to isolate the MOSFET gate drive to prevent unbalancing the strain-gage circuit. Figure 10 shows the circuit arrangement used to drive the power MOSFET and isolate it from the rest of the conditioner. The power MOSFET requires a positive pulse on its gate of at least 10 volts to turn it on rapidly. This is produced by a Hewlett-Packard Type HCPL-2211 optical isolator (Ref. 4) which has a totem pole output and will operate with V_{cc} voltages from 4.5 to 20 volts. The dc-dc converter is a Burr-Brown Type 700 (Ref. 5) and requires an input of 15 vdc and has an input-output capacitance of only 3 pF. The optical isolator is driven from a square-wave source in the conditioner. Exact amplitude of the drive is unimportant as long as it will turn on the LED of the isolator; calibration accuracy is controlled by the 390-ohm R_{CAL} resistor.

The delta-R calibration scheme may also be used to perform an end-to-end verification check on a stress channel. The voltage-substitution calibration technique will not work for this check because it will still produce a believable calibration signal with an open gage. The square-wave calibration signal also will detect abnormalities in the frequency response of the measurement system. For example, rounding of the leading edge of the square wave will indicate poor high-frequency response; droop or tilt in the top of the waveform would indicate poor low-frequency response.

2.3 DRIVEN SHIELD TECHNIQUE FOR IMPROVED COMMON-MODE REJECTION

The common-mode rejection of a signal conditioner is adversely affected by any unbalance in the resistance of the signal leads such as that caused by the use of thermocouple lead wire with unequal lead resistances. The unbalanced resistance, combined with the capacitance to ground of the cabling between the sensor and the conditioner, has a serious impact on the common-mode rejection at higher frequencies (see Fig. 11). Noise and other undesired signals are coupled as a common-mode signal into the sensor circuit. Because of the cable capacitance, the unequal lead resistances cause unequal portions of this common-mode signal to be fed to the positive and negative instrumentation amplifier inputs, producing a normal-mode signal.

Table 1 shows this effect. A 1.0-v common-mode signal is fed from unbalanced resistances of 100 and 140 ohms through a 100-ft two-wire shielded cable into an instrumentation amplifier. With a cable (Belden 8451) having a wire-to-wire capacitance of 34 pF/ft and having a wire-to-shield capacitance of 67 pF/ft, the resulting normal-mode signal at various frequencies is as shown in Table 1. For illustration purposes, the shield is shown connected directly to ground; normally, there is some impedance between the shield input and the amplifier ground.

The procedure recommended by signal conditioner manufacturers to circumvent this problem is to tie the cable shield to the source of common-mode voltage at the sensor end of the cable so that the shield acts as a guard between the sensor leads and earth ground. With the same common-mode voltage on the signal leads and the shield, there is no difference in potential between one side of the cable capacitance and the other, and the capacitance effectively disappears. Equal common-mode signals are then present on the instrumentation amplifier's positive and negative inputs.

The problem in the real world is locating a single point that truly represents the entire source of common-mode voltage and connecting the shield to it. A solution to the problem, frequently discussed in application notes and other literature (Refs. 6-10) but rarely seen in practice, is to drive the input cable shield with a common-mode signal derived from the input to the amplifier. Two equal-value resistors are connected as a summing network between the positive and negative inputs of the instrumentation amplifier as shown in Fig. 12. The junction of the two resistors then goes to a unity-gain, wideband buffer amplifier that drives the cable shield.

Attempts to incorporate the driven shield technique in the signal conditioner were fruitless. The technique could be made to work under certain conditions and did effectively improve the common-mode rejection of the conditioner. It was found, however, that if the sensor was grounded either intentionally or accidentally, the guard driving circuit became unstable

and oscillated under certain conditions. It was felt that the likelihood of a strain gage becoming grounded was quite high and that the resulting high-frequency oscillations might easily couple into adjacent stress channels. No way was found to work around the problem.

Since driving the shield with a signal derived from the input leads is not possible, the shield should be tied to the test article or the test stand. Although this connection will not include all common-mode signals that are picked up on the input cabling by electrostatic or electromagnetic coupling, it will compensate for common-mode voltages capacitively coupled to the gage and its wiring from the test article. This is preferable to leaving the shield floating at the test stand end of the cable.

3.0 PROTOTYPE SIGNAL CONDITIONER

3.1 BLOCK DIAGRAM

A prototype signal conditioner was built having the circuitry shown in the block diagram of Fig. 13. The conditioner is an assembly of two printed circuit boards that plugs into the power supply board of a Pacific Instruments Model 8202 mainframe.

The input board, shown at the top of Fig. 13, includes a low-noise excitation supply and an instrumentation amplifier that float at the common-mode potential existing on the input cabling. The board includes the lead-resistance correction resistors and their control circuitry as well as the delta-R calibration circuit. The instrumentation amplifier has a fixed gain of 100X, and amplifies the signal to improve the ratio of signal to common-mode voltage before the resultant is fed to the output board.

The output board shown at the bottom of Fig. 13 has an instrumentation amplifier on its input to remove the common-mode component of the signal coming from the input board. This amplifier has switch-selectable gains in binary steps from 4X to 128X. The instrumentation amplifier is followed by a 4-pole Bessel low-pass filter. Plug-in resistors are used to select cutoff frequencies from 10 kHz to 100 kHz. Unity-gain current amplifiers provide two buffered outputs from the conditioners. Maximum full-scale output is ± 10 volts.

The power supply in the Pacific Instruments Model 8202 mainframe was modified to provide the voltages necessary for operation of the conditioner. These modifications are described in detail later.

3.2 MECHANICAL DESCRIPTION

The prototype signal conditioner was designed as a plug-in module for a Pacific Instruments Model 8202 mainframe. These mainframes include the necessary power supplies for transducer

excitation and amplifier power and mount in a 5¼-in.-high by 19-in.-wide rack mount. Use of the Pacific mainframe simplifies the mechanical packaging of the prototype conditioner and provides a low-noise, triple-shielded power transformer for the excitation supply in the conditioner.

The arrangement of the two printed circuit boards making up the conditioner is shown in Fig. 14. The output board plugs directly into the power supply card of the Pacific 8202 and has the conditioner front panel attached to it.

The input board is mounted on insulated standoffs above the output board. A guard shield, consisting of a plane on the back side of the PC board and a copper sheet mounted on insulated standoffs above the component side of the board, surrounds the input board.

A 16-wire flat cable with DIP plugs on each end is used to route power and control wiring between the two PC boards. Data and calibration signals between the boards are run on separate RG-174/U coaxial cables.

3.3 DETAILED CIRCUIT DESCRIPTION

The complete circuit of the conditioner is shown in Figs. 15-19. Figures 15 and 16 show the input board and Figs. 17-19 show the output board.

Figure 15 shows the calibration and lead-resistance correction circuitry. J1 is a Molex-type connector for a two-conductor shielded input cable coming directly from the rear connector of the conditioner. TP1 and TP2 are input test points on the front panel. Each lead-resistance correction network consists of a 150-ohm resistor and two EG&G Vactec Type VTL5C4 devices in parallel. These are VT1, VT2, R1 and VT3, VT4, R2. Resistors R22 and R23 are ballast resistors fed from the +15v and -15v supplies of Fig. 15. The Analog Devices Type AD524 instrumentation amplifier U1 picks off the input signal through a-c coupling capacitors C1 and C2 and drives a length of RG-174/U miniature coaxial cable going to the output board.

For calibration of the strain-gage system, power MOSFET transistor Q1 shunts calibration resistor R5 across a 10-ohm resistor in series with the lower lead from the strain gage. A corresponding 10-ohm resistor is placed in the upper strain-gage input lead to maintain circuit balance. The MOSFET is driven with a square-wave calibration signal from the output board through a Hewlett-Packard Type HCPL-2211 optical isolator IS01. The output of the HCPL-2211 is a totem pole type which rapidly drives the capacitive input of the MOSFET in each direction to reduce the width of any switching spikes that may be coupled through to the output of the MOSFET. Schottky diode D1 clips any remaining spikes on the MOSFET

output. The dc-dc converter is a Burr-Brown Type 700. This supply has a very low input-to-output capacitance and is completely shielded. The output is taken between the positive and negative terminals rather than between the positive terminal and ground to help balance out the 160-kHz ripple coupled to the output of the supply. The dc-dc converter is fed with 10 vdc from LM317 regulator U4, and the converter has an output of 20 vdc. An Aromat Type AQV202 optical switch IS02 turns the dc-dc converter on only during calibration to keep any remaining 160-kHz ripple from appearing on the stress signal.

The lower AD524 (U2) and the UA723 (U3) comprise the control circuit for the variable resistances. The d-c voltage on the gage side of the ballast resistors is picked off by the AD524 instrumentation amplifier U2 and converted to a ground referenced voltage. The network R9, R10, R11 divides the voltage by a factor of three to prevent overloading the AD524. Under normal operation there should be 12.6 vdc at the input to the network. The output of the AD524 is fed to one of the inputs of the comparator amplifier in the UA723 regulator chip. The reference input to the UA723 comes off a voltage divider (R18 and R19) from +15 vdc. This voltage divider may be used to set the excitation current through the gage. The output power transistor of the UA723 drives the current through the LEDs of the Vactec devices to control the resistance of their photoconductive cells. Capacitor C10 on the compensation terminal of the UA723 limits the bandwidth of the control loop to less than 1 Hz so that the loop will respond only to the slowly changing lead-wire resistance changes and not to the rapidly varying gage resistance changes.

A network consisting of IS03, IS04, D3, R13 across the excitation leads detects an open circuit in the gage or its wiring. If an open is detected, a light on the front panel of the conditioner changes color from green to red and the resistance control loop is disabled by IS04. Disabling the control loop eliminates having the LEDs of the Vactec devices being driven hard on for long periods of time when the conditioner is powered up but no gage is connected.

Optical switch IS05 is used to disable the control loop whenever the excitation removal circuit (described later) is actuated.

Figure 16 shows the low-noise ± 15 -vdc excitation supply. This supply is powered with ± 20 vdc from the Pacific power supply. An LT1021 precision voltage reference (U9) generates 10.000 vdc which is amplified by a factor of 1.5X by OP227 (U6) and LT1010 (U5) to provide the +15-v excitation. The +15 vdc is then inverted by OP227 (U8) and LT1010 (U7) to provide the -15-vdc excitation. U5 and U7 are current buffers.

Voltage regulators U10 and U11 supply the ± 15 vdc to instrumentation amplifiers U1 and U2 of Fig. 15. Optical switch IS06 shorts the input to the 10.000-vdc reference when the excitation removal circuit is actuated.

Figure 17 shows the amplifier circuitry on the output board. U12 is a Datal Type AM543 programmable-gain instrumentation amplifier. Switch SW1 selects binary gain steps 4X through 128X. A Fairchild diode matrix (D6) encodes the switch positions in binary for the AM543. Potentiometer R37 provides the input zero adjustment on the AM543, and R38 is the output zero adjustment.

LF356 operational amplifier U13 is a unity-gain buffer that provides a low output impedance to drive the 4-pole Bessel low-pass filter composed of LF356 op amps U14 and U15. The filter cutoff frequency is set by plug-in resistors R40, R41, R43, R44. With the capacitor values shown for C36, C37, C40, C41, the cutoff frequency ranges from 10 kHz with 10k resistors to 100 kHz with 1k resistors. Test points TP3 and TP4 are available on the front panel of the conditioner to monitor the output signal.

U16A/U17 and U16B/U18 are unity-gain buffer output drivers. The outputs are designed to provide ± 2.5 vdc or peak ac but can be driven as high as ± 10 vdc. Resistors R51 and R54 may be installed to match the impedance of a transmission line or for ESD protection.

Figure 18 shows the calibration control circuitry. U19 is a type CD4060 and is a combination crystal oscillator and frequency divider. The 1.024-MHz signal controlled by crystal X1 is divided down to 1 kHz. When SW2 on the front panel is raised to the CALIBRATE position, the oscillator/divider is energized and a 1-kHz square wave is applied to isolator IS01 on the input board through 74C906 drivers U20A/B. External calibration signals are input through a Burr-Brown Type INA117 instrumentation amplifier. Although designed for a nominal 1-v rms calibration signal, this input will accommodate calibration signals having a wide range of amplitudes. The LM393 dual op amp U23 is a Schmidt trigger used to square up the input signal. R56, D7, R57 shift the +15-vdc level from U23 to match the +5-vdc input level of the CMOS 74C00 AND gate U22B. When a TTL level is applied between the CAL+ and CAL1 inputs, a square wave at the frequency of the external calibration signal is applied to IS01.

The 74C906 drivers U20C/D control optical switch IS02 on the input board to energize the dc-dc converter whenever internal or external calibration is actuated. Whenever either switch SW2 is depressed to the EXCITATION REMOVAL position or a TTL level is applied between the CAL+ and CAL2 inputs, 74C906 drivers U20E/F drive optical switch IS06 on the input board to reduce the excitation voltage to zero.

Figure 19 shows the +15-, -15- and +5-vdc regulators for power to the output board. Input to these regulators is ± 30 vdc from the Pacific power supply board. The LM6321 U25 drives the guard on the secondary excitation and bias supply windings of the power transformer on the Pacific board. LM6321 U26 drives the guard shields on either side of

the input board. Op amp LM358 (U27) is used as a comparator to sense a gage open condition from the input board and drive dual LED D10 green for gage intact and red for gage open.

3.4 MODIFICATIONS TO PACIFIC POWER SUPPLY BOARD

To use the power supply in the Model 8202 mainframe, several modifications to the Pacific power supply PC board are required (see Ref. 11):

1. Components in the regulation circuitry for the transducer excitation supply are removed, and the output of the three-terminal regulators U4 and U5 is connected directly to the output connector. Components removed include R1, R2, R5-R18, C3, C20, Q2-Q4, U1-U3, VR1, and the V/I jumpers. The regulators then are tied to the output by a jumper from U1 pin 4 to the end of R18 connected to J1 pin 30 and a second jumper from U3 pin 7 to the end of R17 connected to J1 pin 32.
2. The values of the voltage setting resistors R20 and R21 on U4 and U5 of the excitation supply are changed to provide ± 20 -vdc output. R20 is changed to 3.48k 1 percent and R21 is changed to 1.74k 1 percent.
3. A heat sink is installed between voltage regulators U6 and U7.
4. Cable assembly W2 is removed.
5. The chassis ground lug is removed from the enclosure guard circuit and connected to the output ground.

4.0 PERFORMANCE OF CONDITIONER

The prototype constant-resistance signal conditioner was tested for excitation regulation accuracy, common-mode rejection, and internal noise. For comparison purposes, measurements of common-mode rejection and internal noise were made on a Neff Instruments Company (Neff) signal conditioning amplifier (SCA) in the constant-voltage excitation mode and on the same Neff SCA with a constant-current regulator built up on a plug-in mode card (Fig. 20).

4.1 EXCITATION REGULATION

Regulation accuracy of the prototype conditioner power supply was determined by measuring the voltage developed across a simulated 120-ohm sensor for different values of

lead wire resistance. The conditioner was set up to supply 30 ma to the sensor and the voltage measured with lead resistances (in each lead) of 0, 20, 40, 60, 80 and 100 ohms. These voltages were then converted to the corresponding gage currents using Ohm's Law.

The results of the measurement of excitation regulation are given in Table 2. The current through the gage changed less than 0.05 percent for the full 100-ohm change in lead resistance. Because of the 1-percent tolerance resistors used in the prototype, the absolute error in setting the gage current to 30 ma was 0.4 percent. The current regulation obtained using the constant-resistance approach is considered very good. The current setting accuracy could be improved by substituting resistors of higher precision, but a high degree of absolute accuracy is not necessary with the delta-R calibration scheme.

4.2 COMMON-MODE REJECTION

Common-mode rejection was measured with a circuit to simulate the actual wiring installation for an engine test (Fig. 21). The two 60-ohm resistors on the input simulate a 120-ohm strain gage. The 40-ohm resistor and the 80-ohm resistor represent typical unbalanced thermocouple wire resistances. The 100 ft of Belden 8451 shielded cable represents the wiring from the test article to the signal conditioner location. Since the common-mode rejection is affected by the capacitance to ground of the input cable and its shield, the cable was wrapped around a metal cylinder connected to the conditioner output ground to control the test conditions. Common-mode rejection was checked at 1, 2, 5, 10, 20, 50, and 100 kHz with each of the three types of conditioners. Low-pass filters in the conditioners were set to 80 kHz.

Common-mode rejection was first measured on the signal conditioners with the sensor cable shield tied to the guard circuit of the conditioner but not connected at the sensor end. This is the customary practice in the AEDC Engine Test Facility (ETF). A second measurement of common-mode rejection was then made with the shield at the sensor end of the cable connected to the common-mode source.

Next, the 40- and 80-ohm resistors simulating the lead-wire resistances were both changed to 60 ohms to provide a balanced configuration, and the above tests were repeated.

The results of the measurement of common-mode rejection are shown in Figs. 22a-d. Generally, the common-mode rejection deteriorates at a rate of 6 dB per octave because of unbalanced input resistances and capacitances. Above about 50 kHz the rolloff of the 80-kHz low-pass filter reduces the amount of signal at the conditioner output, thus improving the apparent common-mode rejection. At low frequencies, the common-mode rejection curve appears to level off when the level of the common-mode signal approaches the internal noise level of the conditioner. Actually, the 6 dB-per-octave slope continues on to below 60 Hz

and could have been measured by increasing the level of the common-mode signal applied to the conditioner or by using a spectrum analyzer to filter the common mode out of the noise.

The inferior performance of the constant-current configuration may be noticed in each of the figures. Also readily apparent is the very poor common-mode rejection obtained when the input cable shield is not tied to the source of common mode.

The plots are in absolute common-mode rejection. Because the three circuits produce a different amplitude signal out for the same amount of strain, these different signal levels must be taken into account when the conditioners' performance is compared. For example, when the constant resistance conditioner is compared to the constant current, the improvement should be decreased by 4.73 dB. When the constant-resistance conditioner is compared to the constant voltage, the relative improvement must be increased by 1.29 dB.

4.3 INTERNAL NOISE

Internal noise comes primarily from the input amplifier and the excitation supply of the signal conditioner and is a function of the bandwidth of the data amplifier. Noise was measured on all three conditioner types using a bandwidth of 80 kHz. The low-pass filter in the Neff SCA is a 6-pole Bessel while the prototype conditioner has only a 4-pole Bessel filter.

Internal noise was measured using the circuit of Fig. 23. Two series-connected 120-ohm metal film resistors were connected directly between the positive and negative signal input pins of the conditioner, and the junction of the two resistors was connected to the guard (shield) input pin. The resistor combination represents a 120-ohm gage with its two wires each having a lead resistance of 60 ohms. The excitation was set to give 30 ma through the gage. The peak-to-peak noise at the output of the conditioner was then measured using a Tektronic Model 2465 oscilloscope with its bandwidth limited to 20 MHz.

The amplitude of the output noise was divided by the gain of the amplifier in the conditioner (800X for the prototype and 256X for the Neff) to give noise in peak-to-peak microvolts referred to the input (RTI). The percent of full-scale signal was next calculated by dividing the RTI value by the full-scale voltage at the input to the instrumentation amplifier and multiplying that value by 100. Full-scale voltage was defined as that resulting from a 0.25-ohm change in a 120-ohm gage (4.35 mv for the constant-resistance circuit, 3.75 mv for the constant-voltage circuit, and 7.5 mv for the constant-current circuit).

The internal noise measured for each of the three conditioners is shown in Table 3. The constant-resistance circuit has a noise level less than that of the constant-current and comparable to that of the constant-voltage conditioner. In addition to the wideband noise

listed in Table 3, the Neff constant-current circuit had 60-Hz spikes having an amplitude of 217 μV peak-to-peak (2.9 percent). These noise spikes are considered unacceptable.

5.0 RECOMMENDATIONS FOR USE OF CONDITIONER

5.1 DATA REDUCTION USING SQUARE-WAVE CALIBRATION SIGNAL

Stress data at the AEDC Engine Test Facility are recorded on analog magnetic tapes using FM multiplex equipment. When these data are reduced, the analog tapes are played back and the stress data are digitized and recorded on digital magnetic tape for entry into high-speed data processing computers. These machines compute the fast Fourier transform on the data and produce spectral plots and Campbell diagrams.

A 1-kHz sine wave calibration signal is recorded ahead of the data on the analog tape. When the tape is played back, a technician measures the rms value of the sine wave using a digital voltmeter. This value is then manually entered into the digitizing system. This voltage reading, along with a previously entered ksi/volts constant, is used by the data processing computers to scale the data.

Because the prototype signal conditioner produces a square-wave calibration signal, a somewhat different method should be used to recover the calibration constant. The peak-to-peak value of the square-wave calibration signal represents a certain amount of stress. Rather than attempting to measure the peak-to-peak value of the square wave, a fast Fourier transform should be calculated using the digitized calibration data. The amplitude of the spectral line at the fundamental of the 1-kHz square wave is then used in scaling the data.

The peak-to-peak amplitude of the fundamental component of a square wave is 1.2732 + times the peak-to-peak amplitude of the square wave (see Fig. 24a). The peak-to-peak value of the 1-kHz component of the calibration signal therefore represents 1.2732 + times the value of stress simulated by the ΔR change in the calibration circuit. For example, if ΔR represents 30 ksi, the amplitude of the 1-kHz spectral line is equivalent to 30×1.2732 , or 38.196 ksi peak-to-peak (see Fig. 24b). If a spectral analysis process is used that produces rms or peak values, the amplitude of the fundamental would be equivalent to $(30 \times 1.2732)/(2 \times 1.4142)$ or 13.504 ksi for rms measurements and $(30 \times 1.2732)/2$ or 19.098 ksi for peak measurements.

By using only the fundamental of the square wave for the calibration, any errors caused by waveform distortion of the square wave are minimized. Rolloff of the leading edge of the square wave or droop in its top will have no effect. Any switching spikes or dc-dc converter ripple coming from the conditioner calibration circuit are eliminated as is any broadband noise or 60 Hz on the calibration signal.

In using this method of determining the calibration constant, one must be careful to use a sampling rate in the analog-to-digital conversion system that will produce a Fourier spectrum having a spectral line at the calibration frequency (1 kHz). Correspondingly, the accuracy of the calibration frequency in the conditioner must be such that the frequency will fall exactly on the spectral line of the FFT processor. (With Hanning weighting, the frequency must be within ± 5 Hz to keep the error from this source less than 1 percent.)

5.2 SETUP OF CONDITIONER FOR DIFFERENT GAGE RESISTANCES AND CURRENTS

The prototype conditioner was initially set up for a 120-ohm strain gage with 30 ma of excitation current through the gage. The use of gages having other resistances or requiring other excitation currents will require the changing of certain circuit components. With a fixed excitation voltage of 30 vdc, current through the gage is determined by the value of the ballast resistors R22 and R23 in Fig. 15. The value for these resistors may be determined using Ohm's Law and assuming that the lead-wire resistance and the lead-correction network total (in each lead) 150 ohms.

Changing R22 and R23 will result in a different voltage at points A and B (see Fig. 6). The voltage divider feeding the reference input of the comparator in the control loop (R18 and R19 in Fig. 15) should be changed to provide a reference voltage equal to one-third of the desired voltage between points A and B. Solder terminals are provided for R22, R23, R18, and R19.

Calibration resistor R5 should be sized for the desired stress calibration level. Its resistance, when paralleled with R4, should generate a ΔR in R4 equal to the gage resistance change for the desired stress.

In analyzing the constant-resistance circuit and in determining the output of the conditioner to expect under different conditions, it has been found useful to use a spreadsheet type of analysis. Different parameters may be varied and the effect on other parameters determined. Table 4 shows such a presentation. The equations for each cell are also given in the table.

5.3 CONDITIONER INPUT WIRING

As discussed in Section 2.3, common-mode rejection is improved significantly by connecting the shield of the input cable to the source of common mode at the sensor. The primary source of common-mode signals for strain gages mounted on the engine comes from the difference between test article ground and conditioner ground. By tying the input cable shield to the test cell, a major contributor to the common-mode signal will be eliminated.

Section 2.3 also describes how common-mode signals are converted to normal-mode signals by the capacitance of the input cabling when there is unequal resistance in the two gage lead wires. All new installations should consider using low-capacitance shielded cables. Low-capacitance cables, such as Belden 89182, having capacitances of 8.8 pF/ft wire-to-wire and 16.5 pF/ft wire-to-shield are now available.

6.0 CONCLUSION

It is possible to improve the accuracy of stress measurement by using new signal conditioning circuits. A prototype strain-gage signal conditioner uses the constant-resistance excitation technique to minimize any effects of lead-wire resistance change. This conditioner maintains a balanced input configuration to maximize the common-mode rejection of undesired high-frequency signals.

The conditioner also includes a delta-R calibration circuit that promises greater measurement accuracy by providing a more direct relation to the actual gage resistance change. This circuit provides an improved means for performing an end-to-end system checkout.

REFERENCES

1. Mahrenholz, Bob G. "An Improved Strain-Gage Signal Conditioner for Dynamic Stress Measurement." Paper No. 91-129, *Proceedings of the 37th International Instrumentation Symposium*, San Diego, CA, May 5-9, 1991, pp. 1115-1129.
2. *Optoelectronics*. EG&G Vactec, St. Louis, MO, pp. 39-48.
3. *HEXFET Power MOSFET Databook*. International Rectifier, El Segundo, CA, 1984, pp. D-97 — D-102.
4. *Optoelectronics Designers Catalog 1988-1989*. Hewlett-Packard, Palo Alto, CA, 1987, pp. 9-15 — 9-18.
5. *Integrated Circuits Data Book*, Volume 33. Burr-Brown Corporation, Tucson, AZ, 1989, pp. 4-86 — 4-87.
6. *Analog IC Data Book*. Precision Monolithics, Inc., Santa Clara, CA, 1990, pp. 6-17 — 6-18, 6-59.
7. *Linear Databook 1*. National Semiconductor Corporation, Santa Clara, CA, 1988, pp. 2-53, 5-58, and 5-59.

8. *The Handbook of Linear IC Applications*. Burt-Brown Corporation, Tucson, AZ, 1987, pp. 142, 154 — 155.
9. *Linear Products Data Book*. Analog Devices, Norwood, MA, 1988, pp. 4-32.
10. Morrison, Ralph. *Grounding and Shielding Techniques in Instrumentation*. John Wiley & Sons, New York, 1986, pp. 161-162 (Third Edition).
11. *Models 8201/8202/8203, Transducer Conditioning Mainframe, Owners Manual*. Pacific Instruments, Inc., Concord, CA.

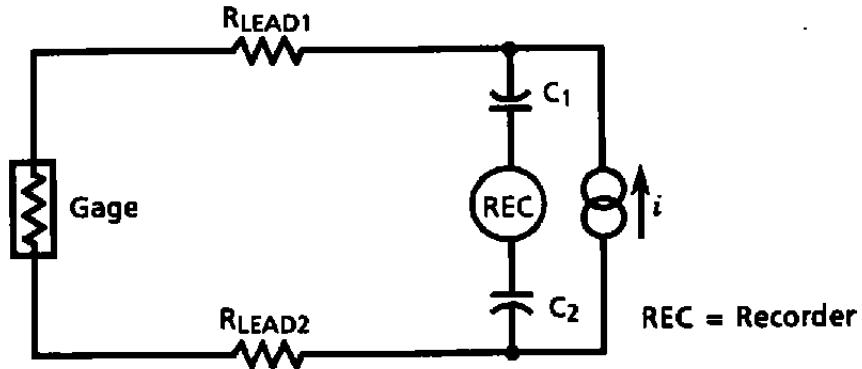


Figure 1. Dynamic stress measurement circuit using constant-current excitation.

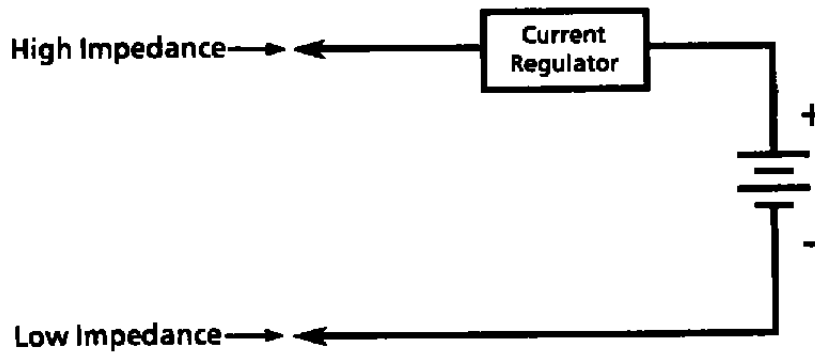


Figure 2. Equivalent of constant-current excitation source.

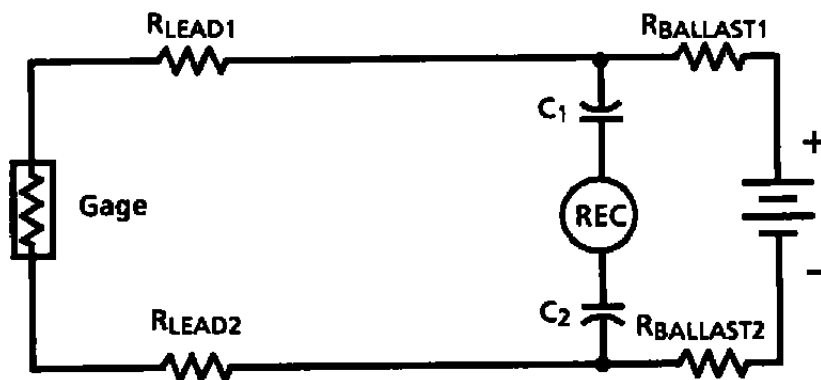


Figure 3. Dynamic stress measurement circuit using constant-voltage excitation.

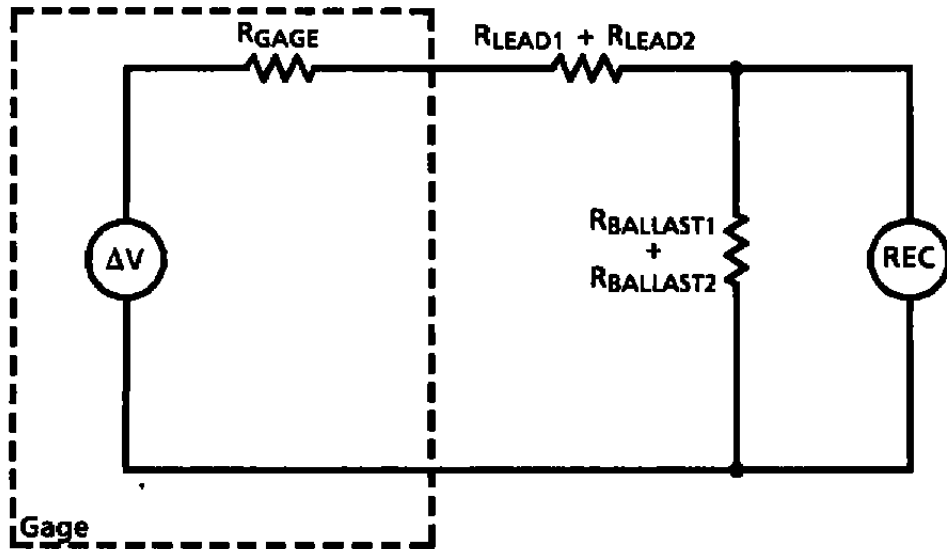


Figure 4. Loading of gage output by excitation supply.

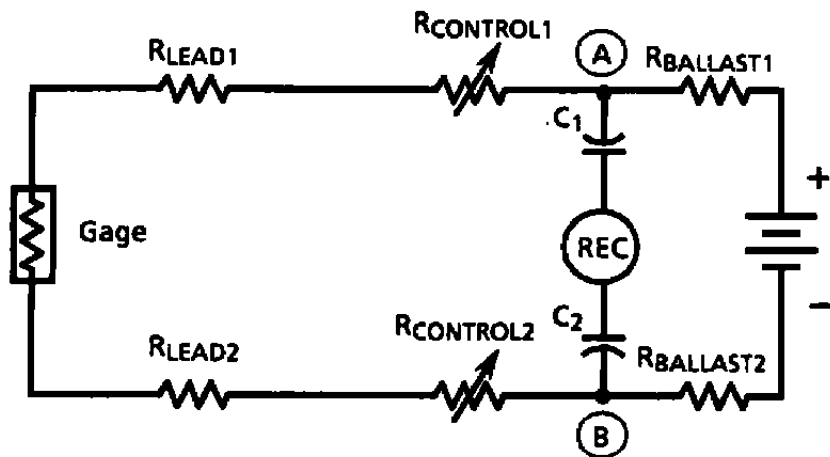


Figure 5. Scheme for lead-wire resistance correction.

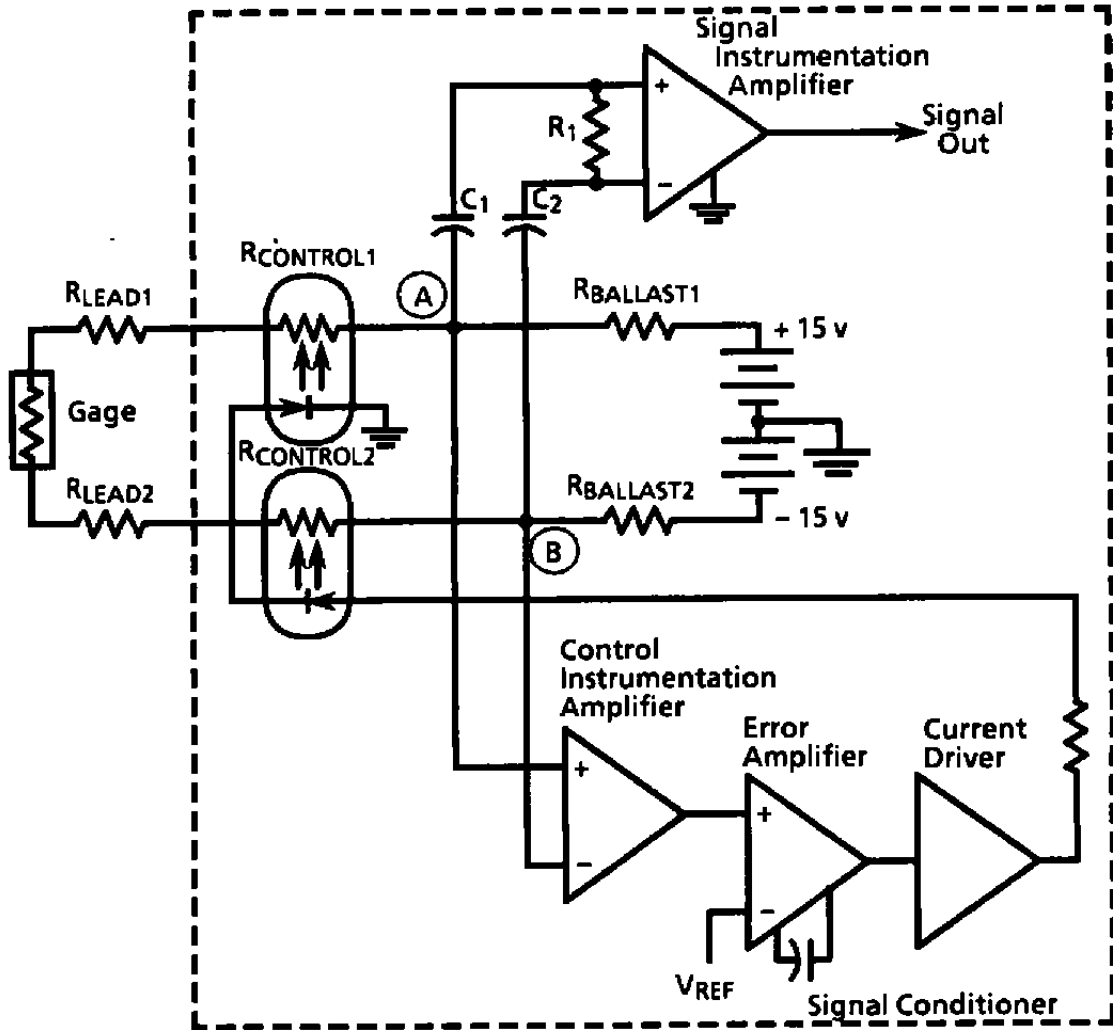


Figure 6. Circuit to correct for lead-wire resistance change.

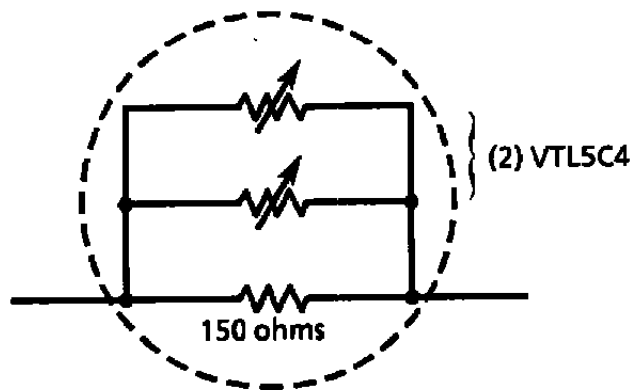


Figure 7. Parallel combination of VACTROLS®.

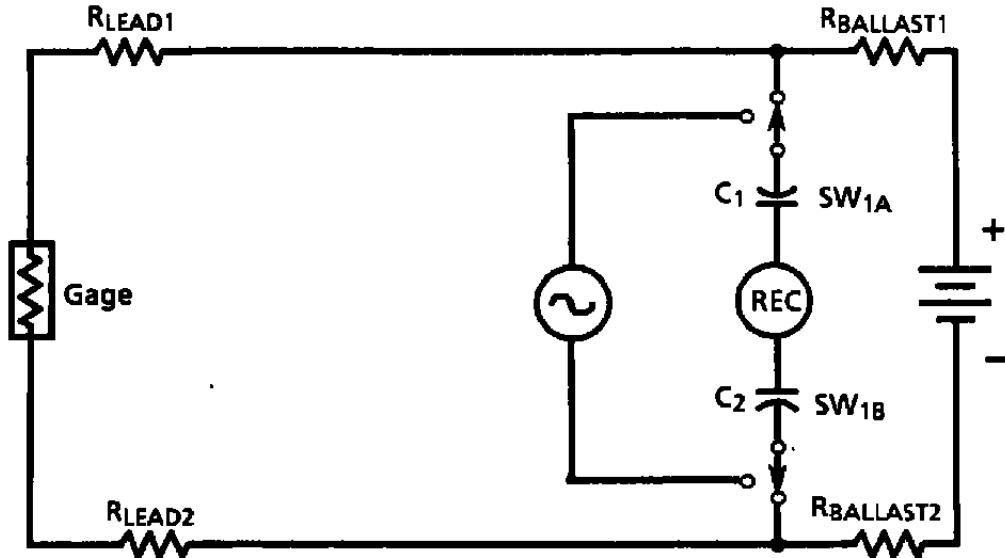


Figure 8. Millivolt substitution calibration technique.

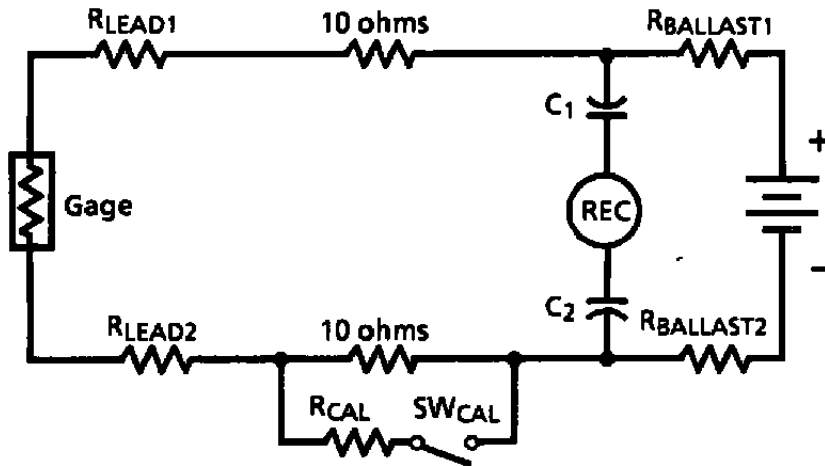


Figure 9. Delta-R calibration scheme.

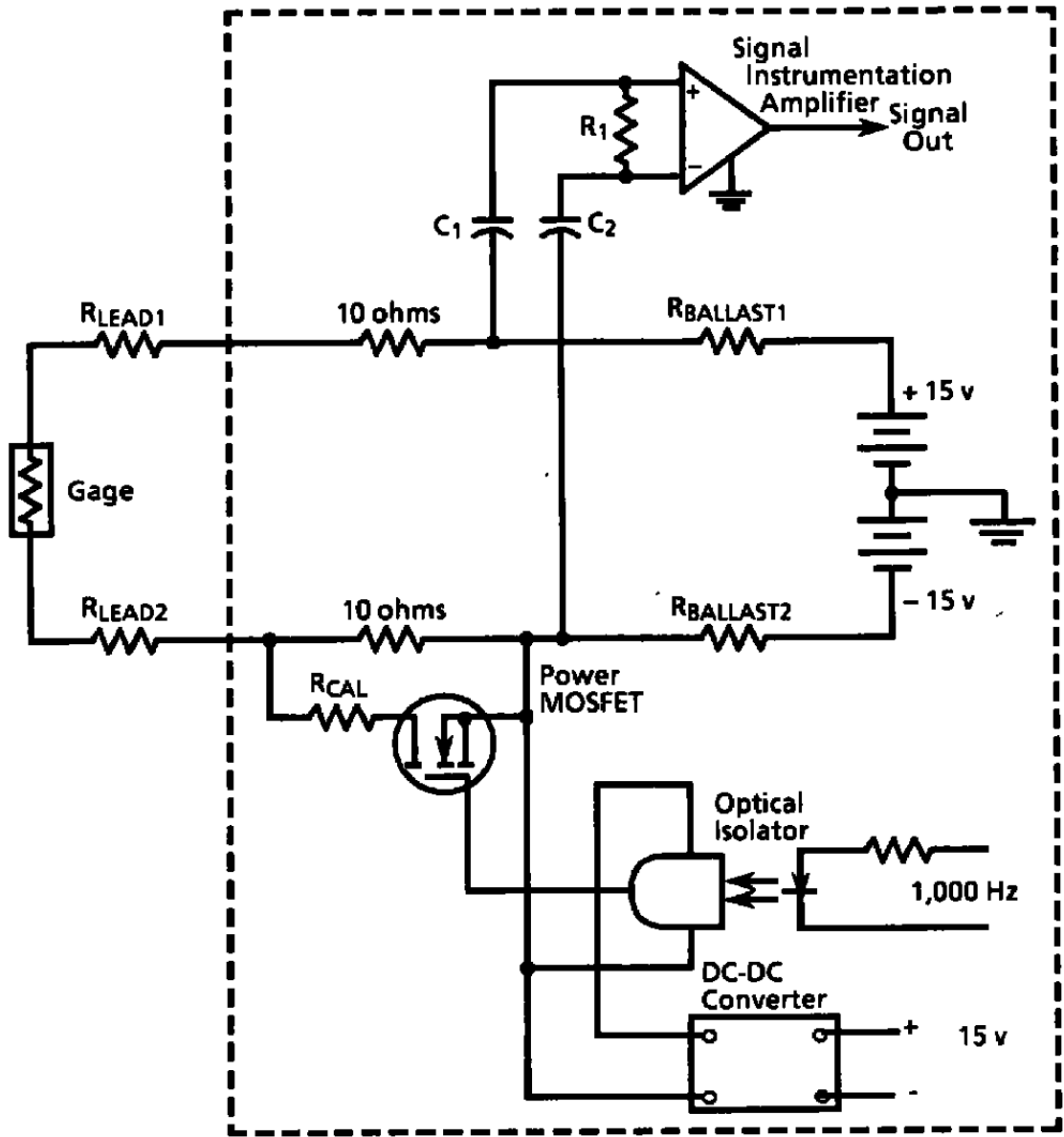
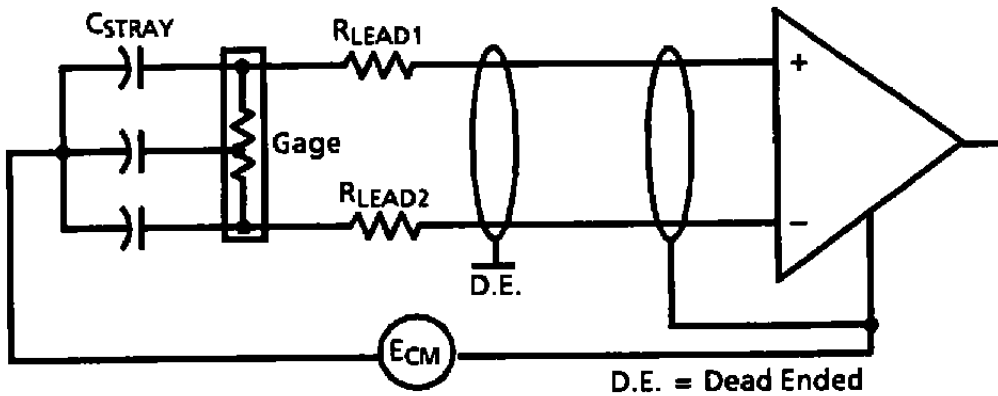
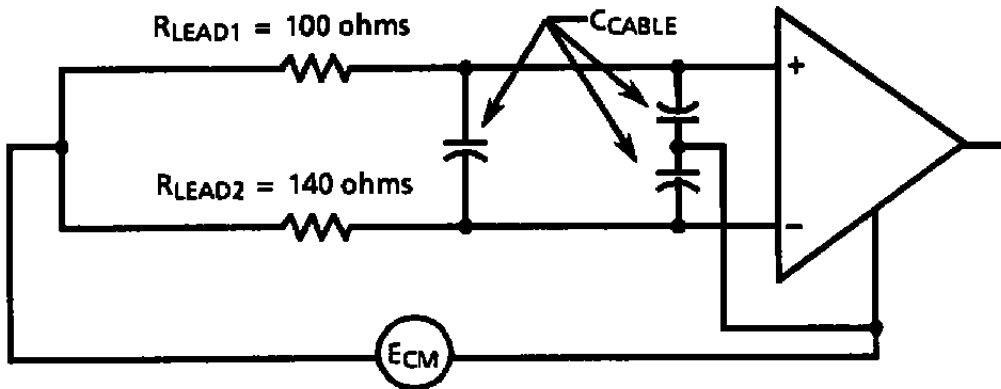


Figure 10. Delta-R calibration circuit using power MOSFET.



a. Actual circuit



b. Equivalent circuit

Figure 11. Effect of unequal lead-wire resistance on common-mode rejection.

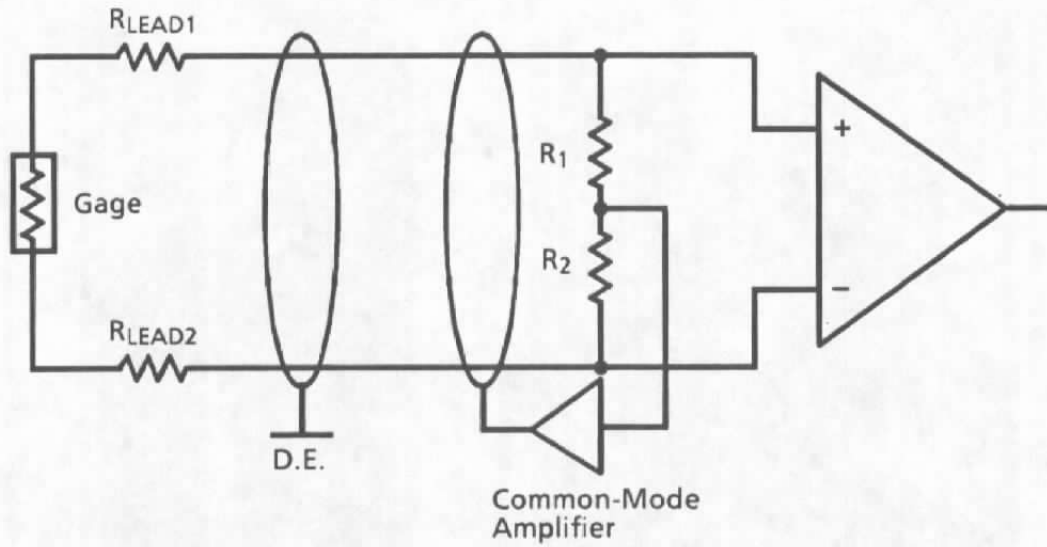


Figure 12. Input cable with driven shield.

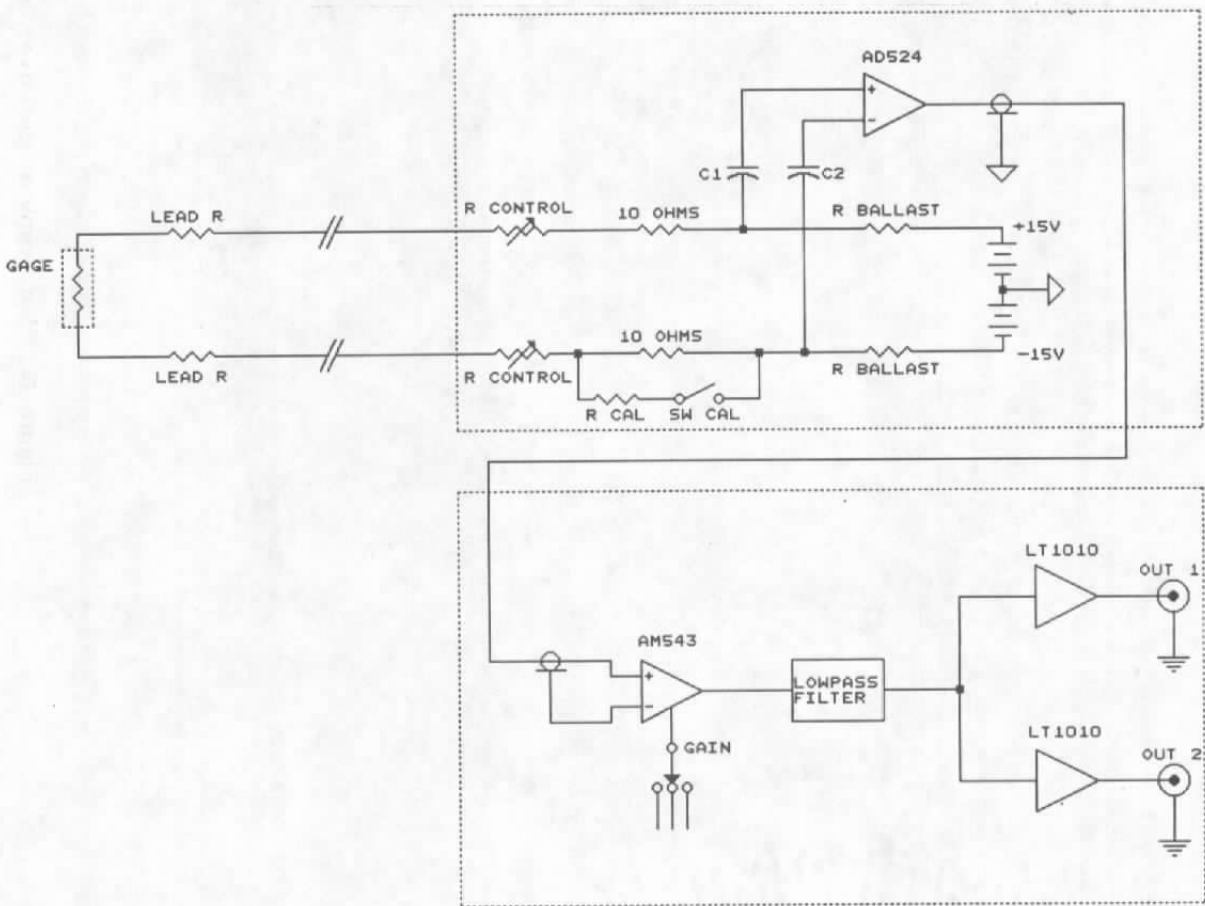
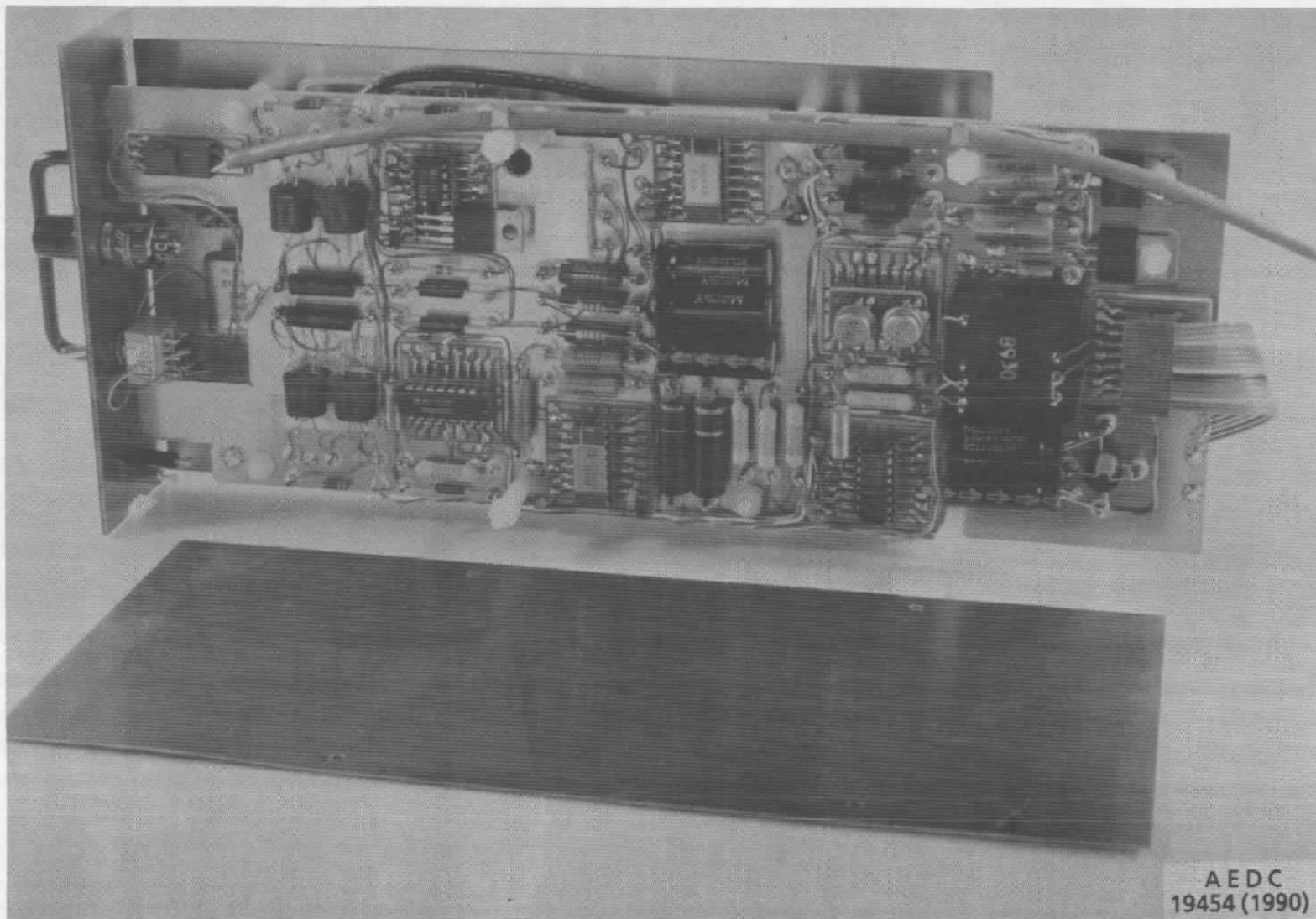


Figure 13. Block diagram of prototype conditioner.



AEDC
19454 (1990)

Figure 14. Photograph of prototype conditioner.

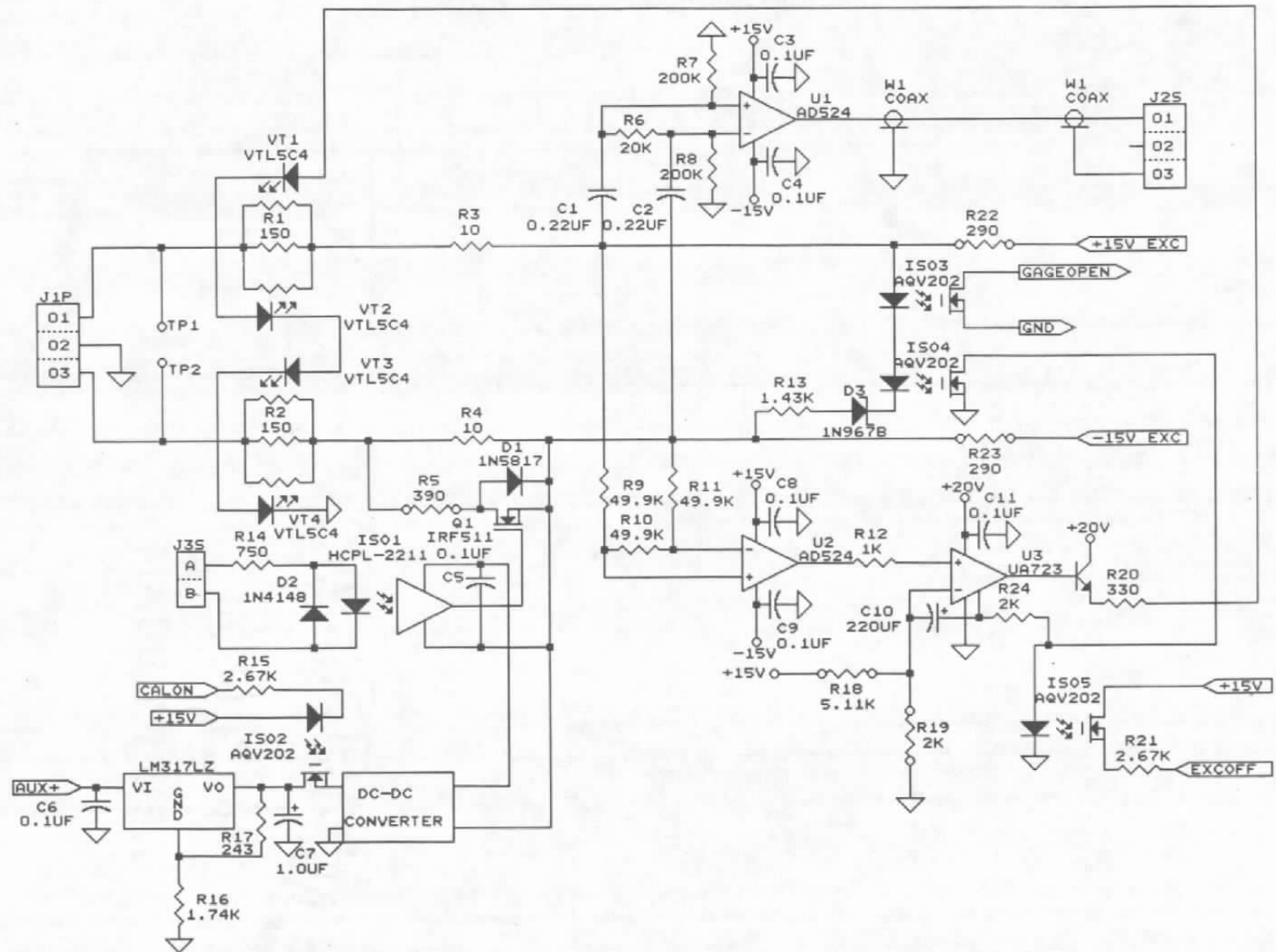
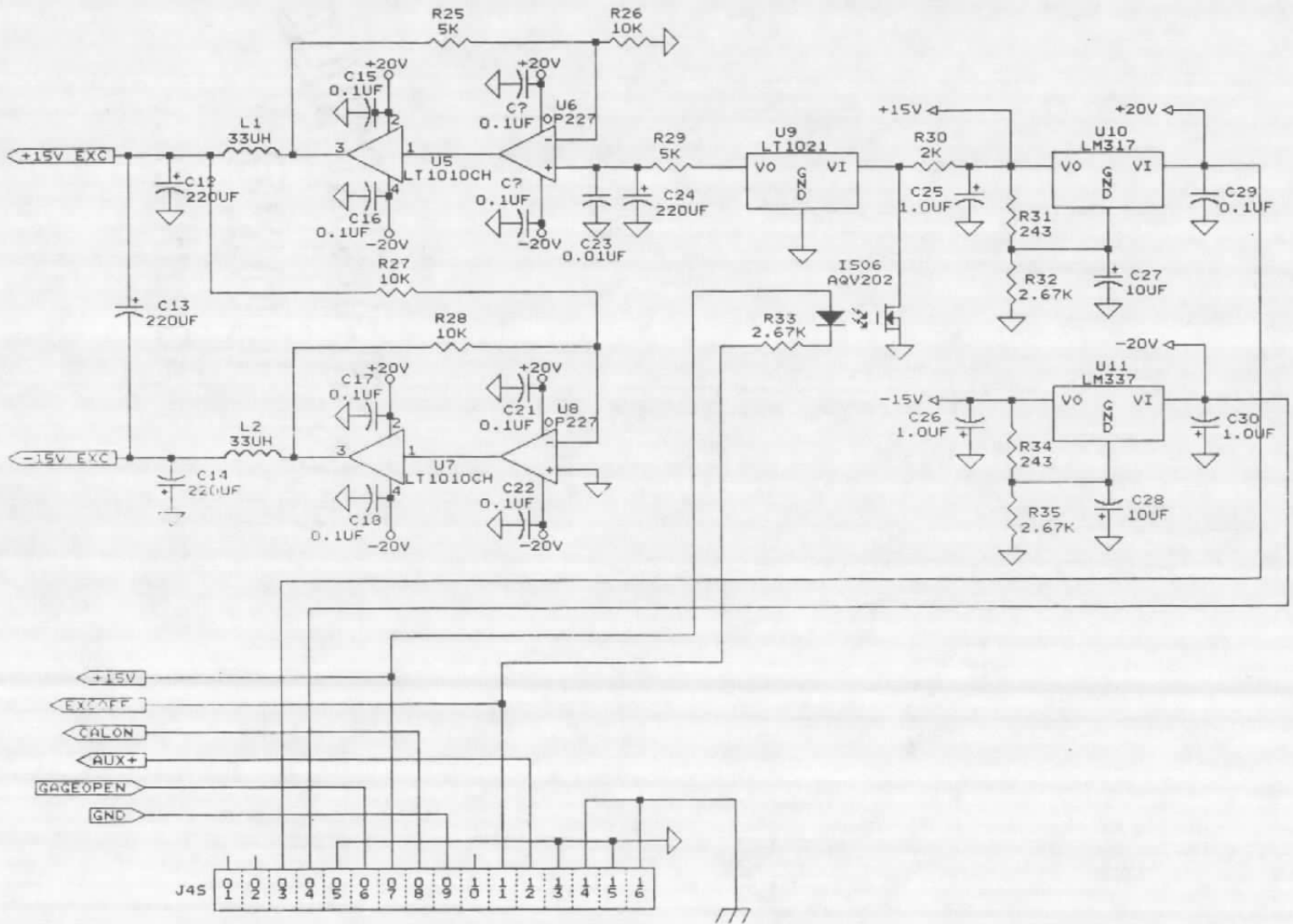


Figure 15. Calibration and lead correction circuitry.



32

Figure 16. Low-noise excitation supply.

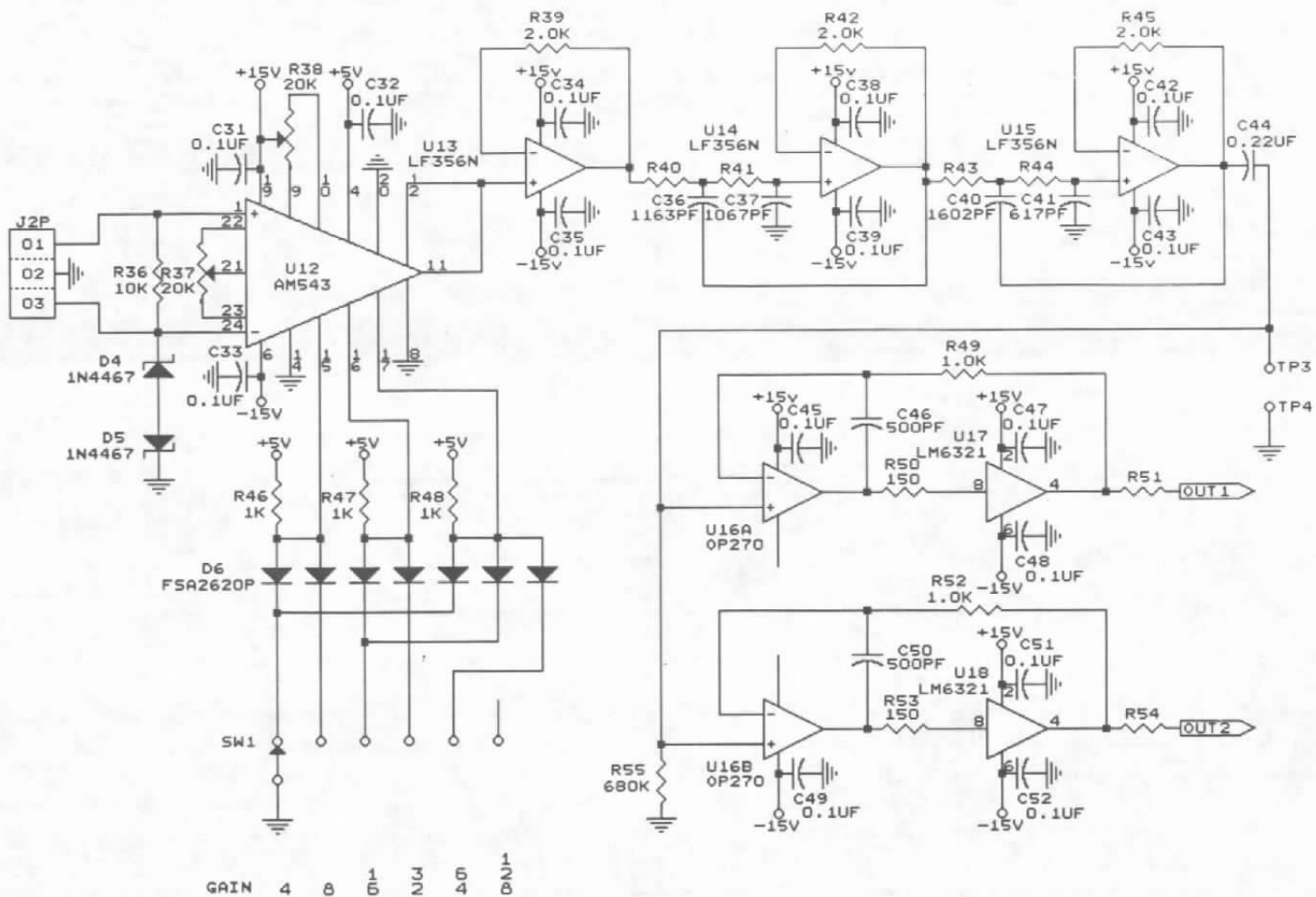
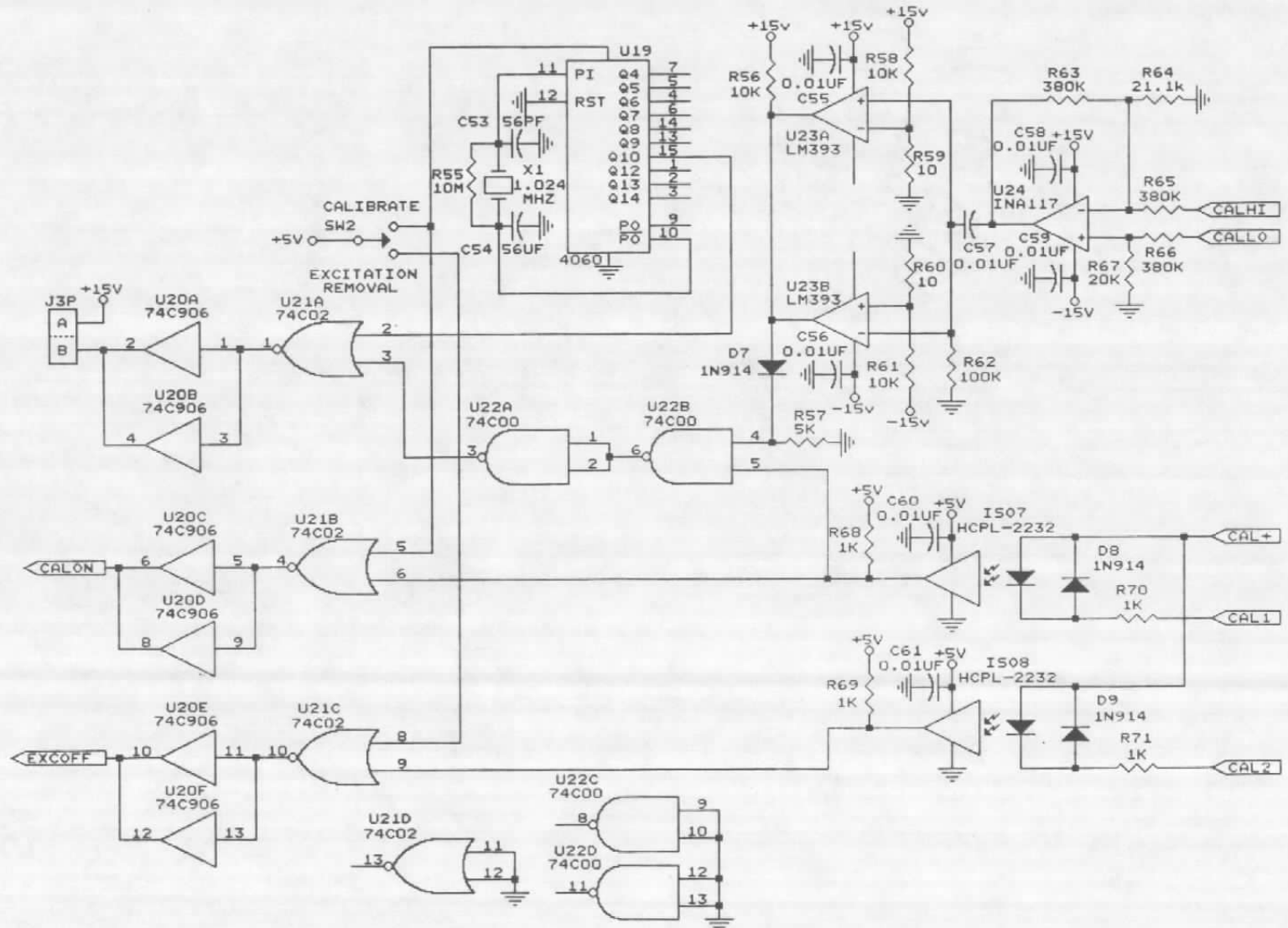


Figure 17. Low-pass filter and output drivers.



34

Figure 18. Calibration control circuitry.

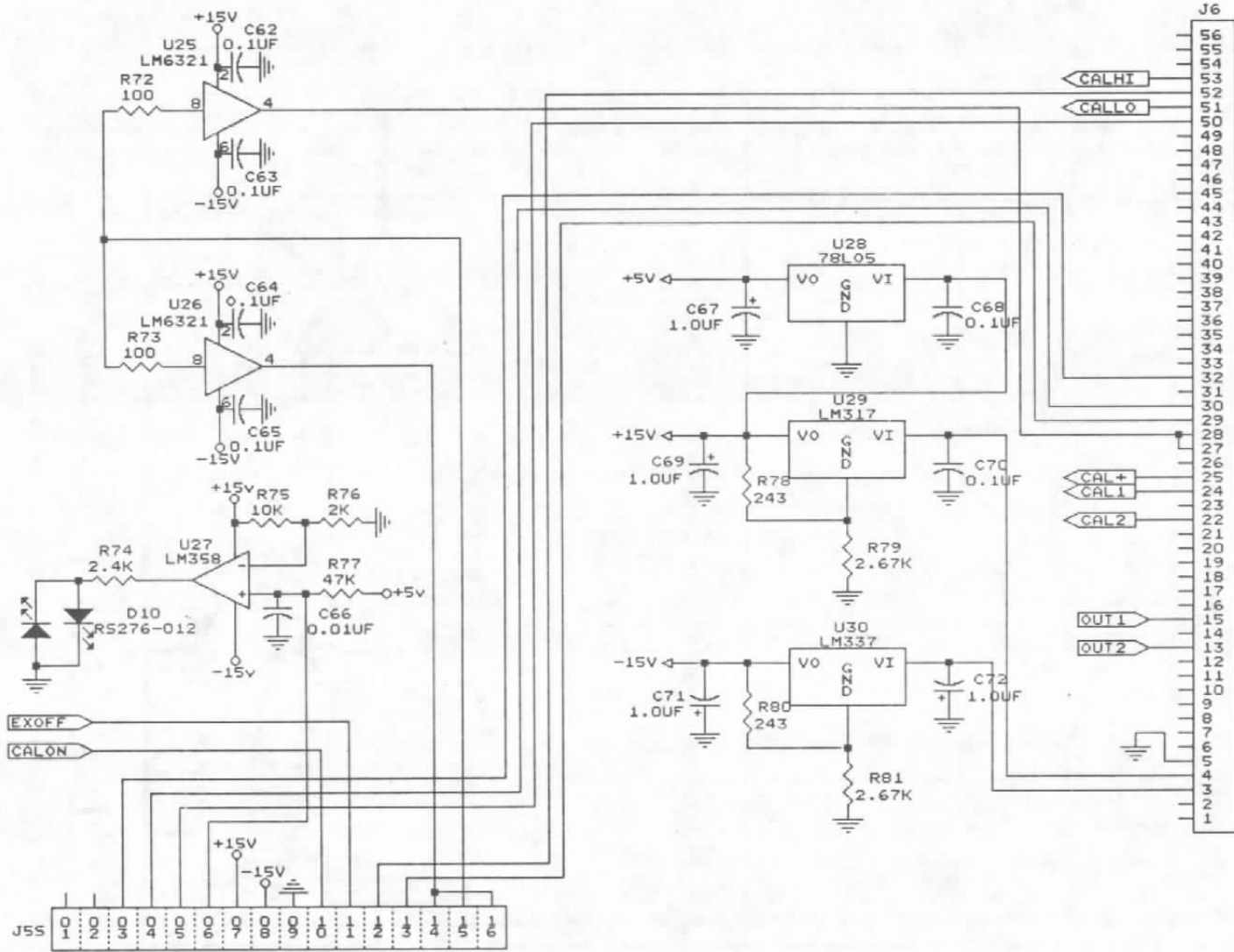


Figure 19. Power connections and guard drivers.

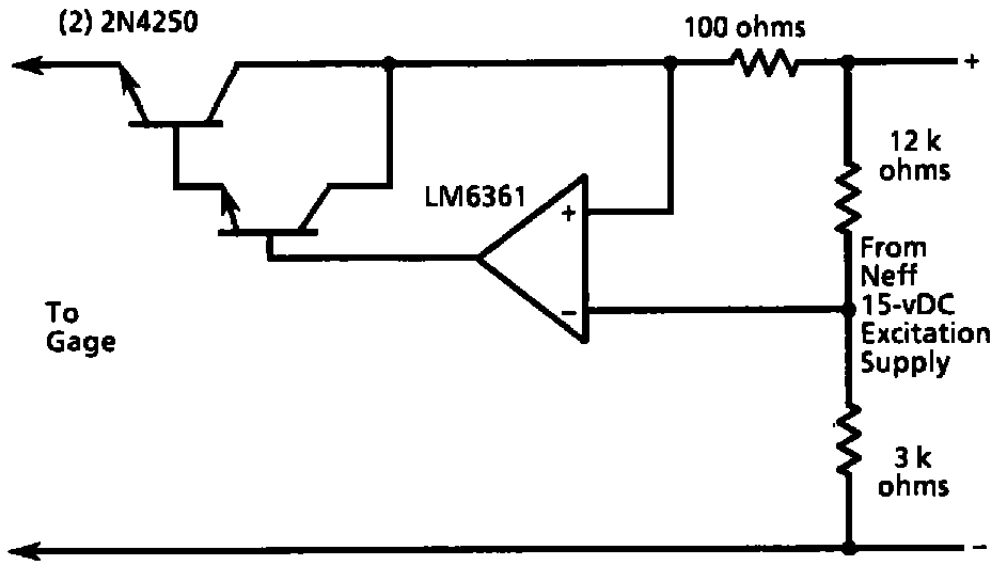


Figure 20. Constant-current regulator for Neff signal conditioner.

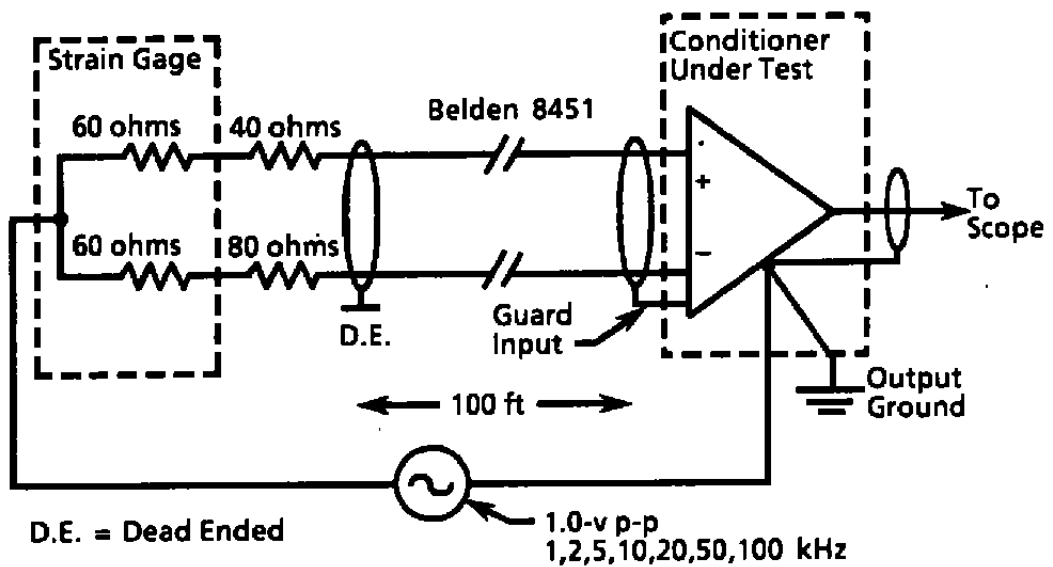


Figure 21. Measurement of common-mode rejection.

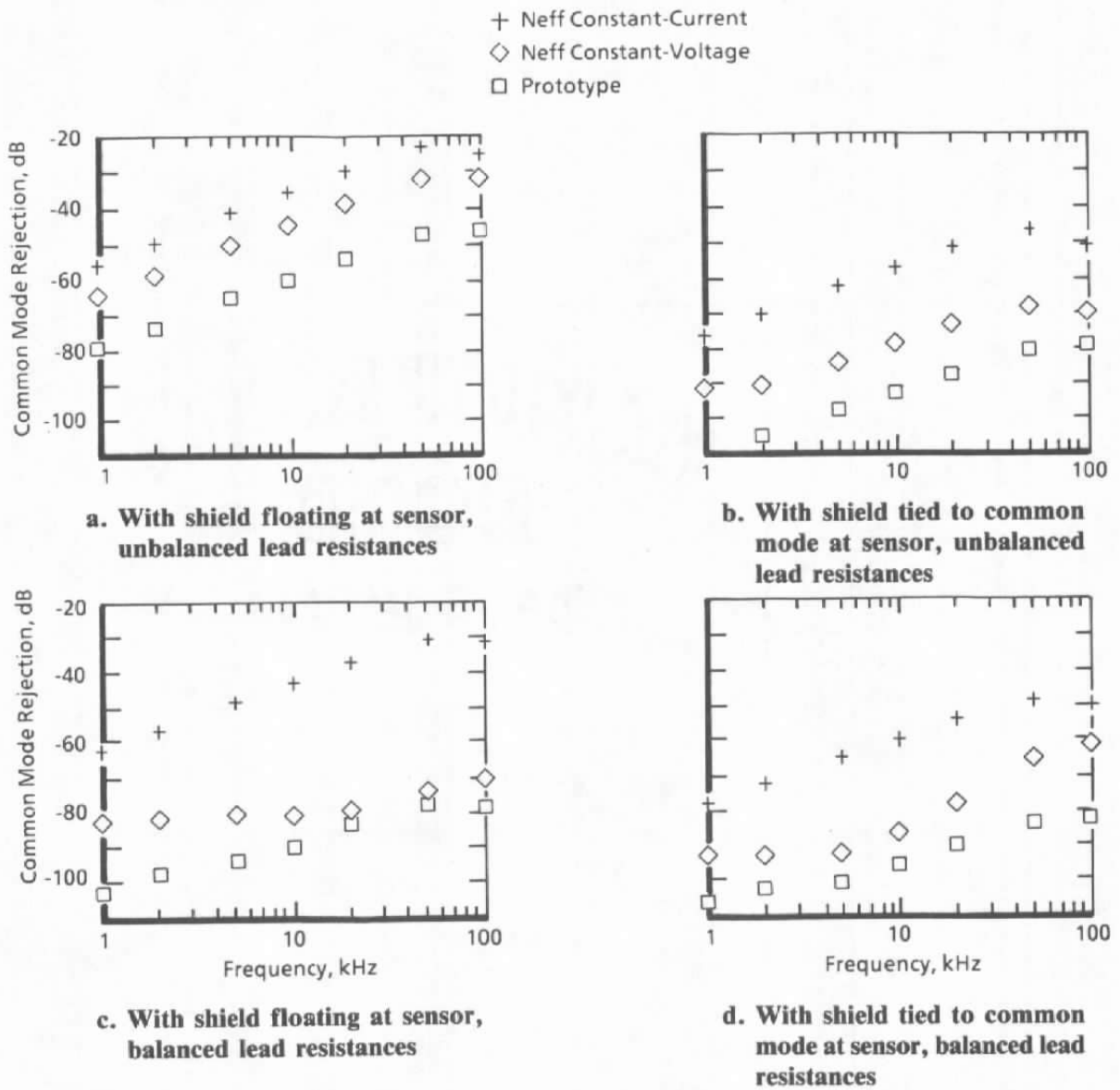


Figure 22. Common-mode rejection.

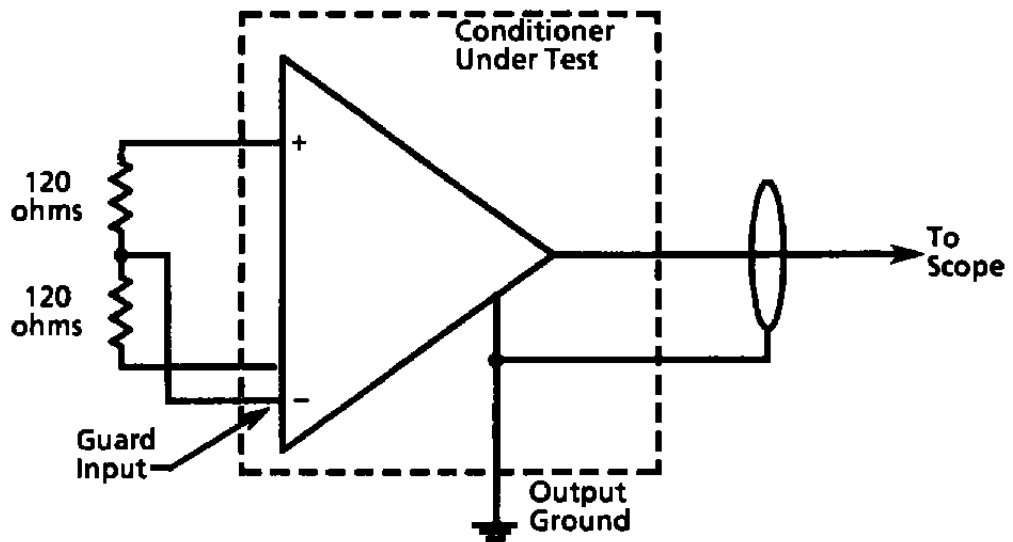
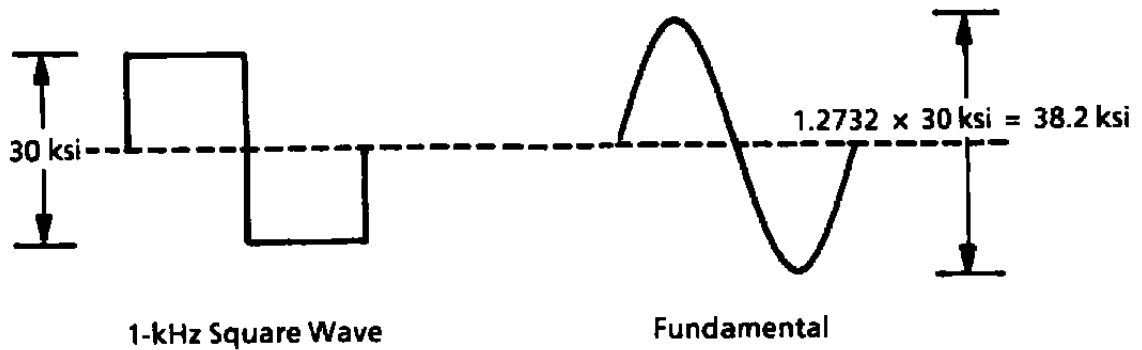
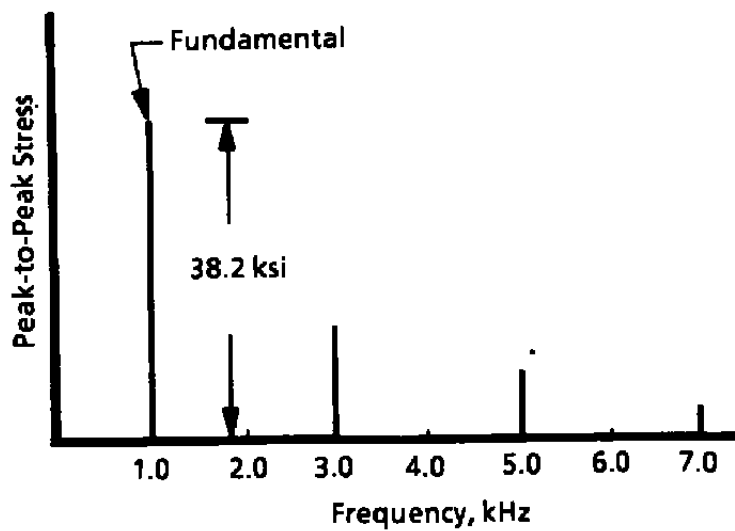


Figure 23. Measurement of conditioner internal noise.



a. Time domain

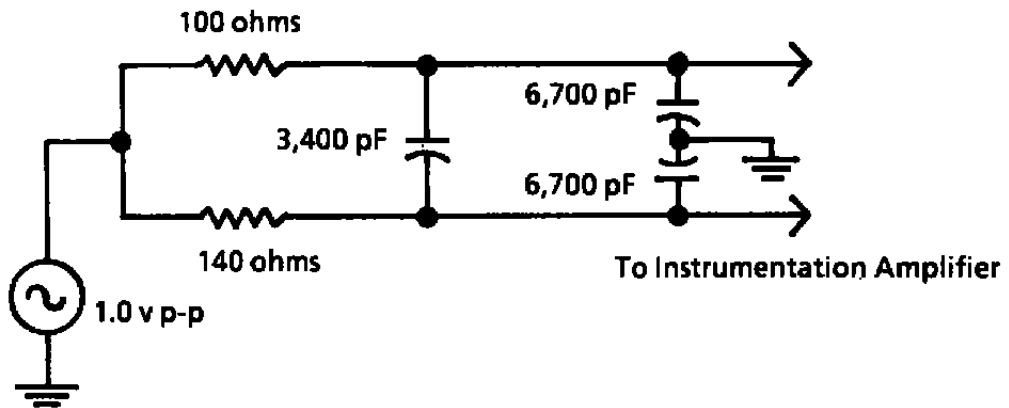


Spectrum of 1-kHz Square Wave

b. Frequency domain

Figure 24. Amplitude of fundamental component of square wave.

Table 1. Common-Mode to Normal-Mode Conversion for Circuit Shown



Frequency	Normal-Mode Signal
100 Hz	0.261 mv p-p
1 kHz	1.693 mv p-p
10 kHz	16.699 mv p-p
100 kHz	104.918 mv p-p

Table 2. Regulation Accuracy

Lead Resistance, ohms	Voltage across Gage, volts	Current through Gage, mA
0	3.5855	29.879
20	3.5854	29.878
40	3.5853	29.878
60	3.5852	29.877
80	3.5849	29.874
100	3.5838	29.865

Table 3. Internal Noise

Constant Resistance F. S. = 4.35 mv		Neff SCA Constant-Voltage F. S. = 3.75 mv		Neff SCA Constant-Current F. S. = 7.5 mv	
RTI	Percent Full Scale	RTI	Percent Full Scale	RTI	Percent Full Scale
41 μ v p-p	0.95	35 μ v p-p	0.94	139 μ v p-p	1.85

Notes:

1. RTI is noise at conditioner output divided by gain of amplifier.
2. Bandwidth of amplifiers is 80 kHz. Neff has a 6-pole Bessel LP filter and prototype constant-resistance has 4-pole Bessel.
3. F. S. assumes a 0.25-ohm change in a 120-ohm gage.

Table 4. Spreadsheet for Analysis of Conditioner

	A	B	C	D
1		RCAL OFF	RCAL ON	
2	RGAGE	120	119.75	---
3	RLEAD1	60	60	---
4	RLEAD2	60	60	---
5	RCAL	390	390	---
6	RBALLAST	290	290	---
7	VSUPPLY	30	30	---
8	R18	10800	10800	---
9	R19	4200	4200	---
10	RCONTROL	80	80	---
11	I	0.03	0.0300075	---
12	VA-B	12.6	12.595649	---
13	MV OUT	---	---	0.0043511
14	AMP GAIN	---	---	800
15	COND OUT	---	---	3.4808702

Formulas:

$$B10 = 0.5 * (((2 * B7 * B6) / (B7 - 45 * (B9 / (B8 + B9)))) - ((2 * B6) + 20 + B2 + B3 + B4))$$

$$B11 = B7 / (20 + B2 + B3 + B4 + (2 * B6) + (2 * B10))$$

$$B12 = B7 - (2 * B6 * B11)$$

$$C2 = 120 - (10 - ((C5 * 10) / (C5 + 10)))$$

$$C11 = B7 / (20 + C2 + B3 + B4 + (2 * B6) + (2 * B10))$$

$$C12 = B7 - (2 * B6 * C11)$$

$$D13 = B12 - C12$$

$$D15 = D14 * D13$$